Infectious Disease Modelling 11 (2026) 854–879

Contents lists available at ScienceDirect

Infectious Disease Modelling

journal homepage: www.keaipublishing.com/idm

Within host dynamics of HPV infection with cellular immunity and HPV-infected dormant cells reactivation

Michael Chapwanya [a,*], Adèle Claire Fouape [a], Berge Tsanou [a,b]

[a] Department of Mathematics & Applied Mathematics, University of Pretoria, Pretoria, South Africa
[b] Department of Mathematics & Computer Sciences, University of Dschang, Dschang, Cameroon

ARTICLE INFO

Article history:
Received 19 June 2025
Received in revised form 21 October 2025
Accepted 26 December 2025
Available online 13 January 2026
Handling Editor: Dr. Jianhong Wu

Keywords:
HPV-Infected dormant cell
Infection reactivation
Cellular immunity
Global stability
Hopf bifurcation
Sensitivity analysis

ABSTRACT

Like other viruses, human papillomavirus genotypes can remain dormant for years or decades and later reactivate due to some well-known factors. The activation of such a dormant infection years later can cause many health and behavioural problems at the individual and societal levels, respectively. From a personalised health perspective, reactivation of a dormant HPV, especially high-risk genotypes such as HPV 16 or 18 can worsen the health condition of the infected person, should they be (or happen to be newly) infected with a different HPV genotype. However, detailed mechanisms that impact the health outcome of an infected person due to rebounding dormant HPV have not been mathematically investigated. The core of this paper is to study the dynamics of an in-host high-risk HPV infection, taking into account cell-mediated immunity and the consequences of reactivation of HPV-infected dormant cells using compartmental modelling. The local and global stabilities of the equilibria are established using Lyapunov and LaSalle techniques, and the bifurcation analysis is performed. Compared to the model without the provision of virus particles due to the reactivation of infected dormant cells, our results suggest that such reactivation can exacerbate the health condition of an infected person by promoting the persistence of infection, which further weakens the active immune response and favours the progression of infection to HPV-induced cancers. In addition, we provide the sensitivity analysis of threshold parameters, state variables with respect to model parameters, and numerical simulations are used to illustrate the theoretical results.

1. Introduction

Human papillomavirus (HPV), which is the main cause of cervical cancer, is a small, non-enveloped, epitheliotropic, double-stranded DNA virus that infects mucosal and cutaneous epithelia and induces abnormal cellular proliferation called cancer. Approximately 200 types of human papillomavirus have been identified and classified in two groups: High-risk (such as HPV 16; HPV 18) and Low-risk (such as HPV 6, HPV 11). HPVs have the specificity that they establish productive infections only within stratified epithelia of the skin, the anogenital tract and the oral cavity.

* Corresponding author.
E-mail address: m.chapwanya@up.ac.za (M. Chapwanya).
Peer review under the responsibility of KeAi Communications Co., Ltd.

https://doi.org/10.1016/j.idm.2025.12.015

Once in a human body, these viruses activate the immune system, composed of two main components that interact with each other to protect organisms from pathogens. The innate response provides a general defence mechanism that can be quickly mounted and consists of macrophages, natural killer (NK) cells and neutrophil leukocytes. The adaptive response lasts longer (up to 7 days) to mount a defence and maintains a memory of pathogens encountered for quick re-activation of the defence if needed in the future. It includes B lymphocytes, T lymphocytes and dendritic cells (DCs). An interested reader is referred to (Mahlbacher et al., 2019; Scott M & Nakagawa, 2001) for more information on the interactions of immune cells with HPVs.

The dynamics of HPV infections and related cancers have been addressed from different perspectives. HPV genomes have been insightfully classified to describe the progression mechanism of infection with each oncogenic genotype to related cancer (Chakraborty et al., 2019; Jensen et al., 2024; Zhou et al., 2023). The work of Mahlbacher et al. (Mahlbacher et al., 2019) gives an overview of tumor-immune continuum modelling approaches, emphasising the effects of immune cells on tumor growth or interactions between immune and tumor cells. The work in (Doorbar, 2023; Westrich et al., 2017) explains how cell dormancy and reactivation can impair the immune defence of the host.

Upon HPV infection, the virus enters the epithelial tissue, moves to the basal epithelial layer (Doorbar et al., 2015) where it stays latent for some time, replicates itself, survives with the help of the host cell, destroys host cellular tissues, and then induces an innate immune response. If this response is inefficient, the persistence of infection can progress from an infectious stage to a precancerous or cancerous stage, in the course of which the adaptive immune system is activated (Carter et al., 1996; Song et al., 2015). For HPV infection, cell-mediated immunity is more important than humoral immunity (Scott M & Nakagawa, 2001).

In fact, cell-mediated immunity is an immune response that does not involve antibodies but rather involves the activation of macrophages and NK-cells, the production of antigen-specific cytotoxic T-lymphocytes, and the release of various cytokines in response to an antigen. Cell-mediated (or cellular) immunity protects the body in three different ways.

First, by activating antigen-specific cytotoxic T-lymphocytes (CTLs) that are capable of destroying body cells displaying epitopes of foreign antigen on their surface, such as virus-infected cells, cells with intracellular bacteria, and cancer cells displaying tumor antigens.

Secondly, by activating macrophages and NK cells, enabling them to destroy intracellular pathogens.

Finally, by stimulating cells to secrete a variety of cytokines that influence the function of other cells involved in adaptive immune responses and innate immune responses. Cell-mediated immunity is directed primarily to microbes that survive in phagocytes and microbes that infect non-phagocytic cells. It is most effective in destroying virus-infected cells, intracellular bacteria, and cancers.

However, while some people clear their HPV infections in a few months, depending on the power of their immune system response, or the vaginal microbiome dysbiosis (Ntuli et al., 2022), others can experience HPV dormancy for decades, possibly the rest of their lives. In fact, HPV, like most viruses, goes through a dormancy period in which it does not cause any symptoms inside or outside the body, and some types of HPV can remain dormant for years before someone develops symptoms or discovers they have it.

On the one hand, there are several reasons why HPV can go dormant, including and not limited to immune system suppression that does not detect the virus; the host-cell interaction during which the host immune system develops tolerance that allows HPV to establish a long-term relationship with its host cells, leading to integration into the DNA of the host cell, making it difficult to detect and allowing HPV viruses to co-exist without causing a host response.

Some factors that cause HPV reactivation include: (1) Chronic stress affects hormonal balance and immune function, creating an environment where viruses thrive. (2) A compromised immune system is one of the primary reasons why HPV becomes active, taking advantage of the vulnerability of a weakened immune system. (3) Hormonal fluctuations/changes also play an active role in HPV reactivation, as women are particularly susceptible during pregnancy or menopause when hormonal levels change dramatically. These shifts can affect immune function and create favourable conditions for viral reactivation.

It is worth noticing that during a dormant or an active HPV infection, the same host can be co-infected with other genotypes of HPV, which may trigger the reactivation of the initial and dormant infection. This process of new infection can happen in many ways, including unprotected or unsafe sexual activities; the acquisition of viruses through external environmental transmission (e.g. nosocomial infection). However, to our knowledge, the later important features of HPV infection have not been mathematically assessed on the dynamics of HPV at the within-host level.

Mathematical modelling is a great tool to predict the long-term behaviour of a given phenomenon. In the case of HPV infections, the review paper of Araujo and McElwain (RP, 2004) proposes the concise contribution of the mathematical modelling in the study of solid tumor growth from the early decades of the twentieth century to 2003. Asih and co-authors in (Asih et al., 2016) used a within-host model to investigate parameters with great impact on the progression of the HPV infection to invasive cancer. Parameters affected by drug treatment and their effect on the risk of cancer progression are also explored. In (Macfarlane et al., 2019), Macfarlane developed discrete and continuous models to describe the competition between different immune cells and tumor-growth to show that there is a correlation between increasing dendritic and/or

cytotoxic T lymphocytes cells number and a decreasing tumor removal time. Smith et al. in (Smith et al., 2013) use a within-host mathematical modelling to predict the long-term outcomes of HPV vaccines.

In this work, we develop a within-host model to evaluate the impact of the production of HPV virus particles due to reactivation of HPV-infected dormant cells on the dynamics of HPV infection, taking into account the immune response and treatment. We perform an in-depth mathematical analysis of the model, proving the existence of equilibria, their local and global stability using Lyapunov-LaSalle's techniques, and sensitivity analysis and numerical simulations. The interpretation of these results suggests that the production of viral particles through reactivation of HPV-infected dormant cells can exacerbate the health condition of an infected human host by driving the persistence of infection, which may further promote the progression to related cancers, even in the presence of an active immune response.

The remainder of the paper is structured as follows. Section 2 deals with the model formulation. Equilibria of the model are determined in the third section, while their local stability/instability, as well as bifurcation analysis, are conducted in the succeeding section. We complete this analysis by investigating the global stability analysis in the fifth section. The sixth Section deals with the sensitivity analysis of state variables towards parameters of the model and simulations that illustrate the theoretical results obtained. The discussion and conclusion section ends the paper.

2. Model formulation

As mentioned above, the immune response is complex and combines innate and adaptive responses. For simplicity and without loss of generality, we aggregate the immune (adaptive) response into a single class D of effective immune cells whose action is to destroy HPV-infected cells. Although this modelling assumption has limitations, it allows us to focus on the main objective of this work, which is to evaluate the role of HPV-induced cell dormancy and reactivation on the dynamics of cervical cancer.

Upon persistent high risk HPV infection, an additional source of HPV viruses within the host level could be provided externally through unsafe sexual intercourse with infected partners, or internally via a reactivation of dormant HPV of the same or different genotype. The biological processes that lead to viral dormancy and reactivation involve the complex interactions between the viral and host cell proteins. Modelling these processes, although important, would amount to describing the various interactions between these proteins at the molecular level and goes beyond the conceptual scope of this work.

Virus latency or dormancy (or viral latency) is the ability of a pathogenic virus to lie dormant (latent) within a cell, denoted as the lysogenic part of the viral life cycle. A latent viral infection is a type of persistent viral infection which is distinguished from a chronic viral infection. Latency is the phase in certain viruses' life cycles in which, after initial infection, proliferation of virus particles ceases. However, the viral genome is not eradicated. The virus can reactivate and begin producing large amounts of viral progeny without the host becoming reinfected by a new outside virus (Doorbar, 2023).

In fact, as highlighted earlier, HPV can remain dormant for a long time, and the maximum duration of its dormancy period is largely unknown and varies from person to person according to human gender, the state of the immune system and life stage. For the simplification of presentation, we choose to model the reactivation of infected cells by considering its direct consequence as the constant provision of free HPV viruses within the infected host, such that it can also be seen as an external source of free HPV viruses due to unsafe sexual intercourse, nosocomial infections, or environmental contamination. However, other birth/recruitment expressions of HPV viruses within the host may be used, such as a bH (linear), bH^n (polynomial): $b > 0, 0 < n < 1$ (Wang et al., 2024), which probably leads to different analytical outcomes and interpretations.

We consider four compartments representing the model's state variables: susceptible or healthy cells denoted by T, infected cells denoted by W, free viruses (or viral particles or virons) denoted by H, and immune defense cells denoted in this work by D; see for example (Mahlbacher et al., 2019; Scott M & Nakagawa, 2001) for more information on the immune cell-HPV interactions. Both innate and adaptive immunity are involved in the clearance of HPV, but in this work, we focus our attention on adaptive cellular immunity. In fact, most HPV viruses are not detected directly by the immune system once within the human body (Senba & Mori, 2012; Song et al., 2015), therefore, adaptive immunity is activated later when cells start to be infected. We let k be the proliferation rate of immune cells (B-lymphocytes, for example) due to infected cells.

When a symptomatic person is screened and diagnosed with HPV infection, the immune system can be boosted or supplemented with a suitable treatment. In some cases, HPV disappears on its own, with no need for treatment. The treatment of HPV depends on the severity of the infection. When the infection persists and causes skin warts, various treatments are possible. These may include the extraction of the wart using salicylic acid or cryotherapy, topical treatment to eradicate the virus, and intervention with a certain type of laser in the event of recurrence. In the case of condylomas, also known as genital warts, these can be treated with medication or medical intervention. In this work, such a feature is taken into account, and we denote by e the efficacy of treatment. The above description can be summarised with the following system of ordinary differential equations:

$$\begin{cases} \dfrac{dT(\tau)}{d\tau} &= \pi - a(1-e)T(\tau)H(\tau) - cT(\tau), \\ \dfrac{dW(\tau)}{d\tau} &= a(1-e)T(\tau)H(\tau) - gD(\tau)W(\tau) - pW(\tau), \\ \dfrac{dH(\tau)}{d\tau} &= f + p\alpha W(\tau) - dH(\tau), \\ \dfrac{dD(\tau)}{d\tau} &= kD(\tau)W(\tau) - \nu D(\tau). \end{cases} \tag{2.1}$$

where τ represents a temporal variable, and the non-negative initial conditions are:

$$T(0) = T^0,\ W(0) = W^0,\ H(0) = H^0,\ D(0) = D^0. \tag{2.2}$$

The schematic transmission diagram of the model is given by Fig. 1.

All parameters in model (2.1) are nonnegative constants, and their biological interpretations are provided in Table 1.

3. Equilibria of the model

In this part, we first investigate the well-posedness of model (2.1) and assess the existence of equilibria. The following theorem deals with well-posedness in terms of existence, positivity and boundedness of solutions.

Theorem 1. *If $T^0 \geq 0, W^0 \geq 0, H^0 \geq 0, D^0 \geq 0$, then the solution $(T(\tau), W(\tau), H(\tau), D(\tau))$ of model (2.1) exists, is non-negative and bounded for all $\tau \geq 0$.*

Proof. We start by proving the existence of solutions. The system of equations (2.1)-(2.2) is a Cauchy problem with the functions defined on the right-hand side of (2.1) indefinitely differentiable with respect to T, W, H and D, therefore, thanks to the Cauchy-Lipschitz theorem, the solution exists and is unique.

Next, we check the positivity of the unique solution guaranteed by the Cauchy-Lipschitz theorem. Let $a_1 = a(1-e)$, $y(\tau) = a_1 H(\tau) + c$;. Without loss of generality, the first equation of (2.1) can be expressed, after eliminating the positive term π on the right-hand side, as an inequality:

$$\frac{dT(\tau)}{d\tau} \geq -y(\tau)T(\tau),$$

from which we have

$$T(\tau) \geq T^0 \exp\left(-\int_0^\tau y(r)dr \right).$$

Then, if $T^0 \geq 0$, then $T(\tau) \geq 0$ for all $\tau \geq 0$.

From the fourth equation of (2.1), we deduce like before

$$D(\tau) \geq D^0 \exp(-\nu\tau).$$

Then, if $D^0 \geq 0$, $D(\tau) \geq 0$ for all $\tau \geq 0$.

Now, we consider the subsystem

$$\begin{cases} \dfrac{dW(\tau)}{d\tau} &= a_i(1-e)T(\tau)H(\tau) - gD(\tau)W(\tau) - cW(\tau), \\ \dfrac{dH(\tau)}{d\tau} &= f + p\alpha W - dH(\tau), \end{cases} \tag{3.1}$$

where $T(\tau)$ and $D(\tau)$ are positive for all $\tau \geq 0$; it can be rewritten as

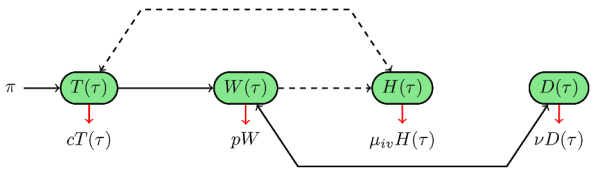

Fig. 1. Flowchart diagram for the transmission process.

Table 1
Model parameters, definitions and estimated values.

Par.	Biological meanings	Range	Units	Refs.
π	Rate at which healthy epithelial cells are produced	[10, 1000]	cell ·day^{-1}	assumed
f	Production rate of virus particles by reactivated dormant cells or from an external source	[0, 1000]	virion ·day^{-1}	assumed
k	Rate of proliferation of immune cells due to the presence of infected cells	[0,3000]	(cell·day)$^{-1}$	Murall et al. (2019)
a	Infection rate of susceptible cells by free virus	[10^{-15}, 1]	(virion·day)$^{-1}$	[12, 16]
e	Efficiency of treatment	[0, 0.9999]		Lee and Tameru (2012)
g	Decay/death rate of infected cells due to immune cells	[1.23, 5.5] $\times 10^{-3}$	(day·cell)$^{-1}$	Abate et al. (2025)
α	The quantity of HPV generated by each infected cell	[10, 10^6]	virion·cell^{-1}	Sierra-Rojas et al. (2022)
c	Apoptosis rate of susceptible cells	[0, 1]	day^{-1}	Murall et al. (2019)
p	Apoptosis rate of infected cells	[0.001, 1]	day^{-1}	[6, 2, 16]
d	Natural death rate of virus	[0.048, 2.5]	day^{-1}	[23, 6]
ν	Immune cell natural death rate	[0.001, 1]	day^{-1}	Gurcan et al. (2014)

$$\frac{dX_i}{d\tau} = A(X)X_i + B, \tag{3.2}$$

where $X = (W,H)^t$, $A(X) = \begin{pmatrix} -gD - c & a_1 H \\ p\alpha & -d \end{pmatrix}$ and $B = (0,f)^t$.

Note that $A(X)$ is a Meztler matrix and $B \geq 0$, therefore, the solution of (3.1) is non-negative (Capasso & Capasso, 1993). We end the proof by proving the boundedness of the solution. Adding the first two equations of (2.1), we obtain

$$\begin{aligned} \frac{d(T(\tau)+W(\tau))}{d\tau} &\leq \pi - gD(\tau)W(\tau) - cT(\tau) - pW(\tau) \\ &\leq \pi - \min\{c,p\}(T(\tau)+W(\tau)). \end{aligned}$$

Therefore, for all $\tau \geq 0$,

$$T(\tau)+W(\tau) \leq \frac{\pi}{\min\{c,p\}} + \left(T^0 + W^0 - \frac{\pi}{\min\{c,p\}}\right)\exp(-\min\{c,p\}\tau),$$

from which we deduce

$$T(\tau)+W(\tau) \leq \max\left\{\frac{\pi}{\min\{c,p\}}, T^0 + W^0\right\}.$$

Let $\overline{M} = \max\left\{\frac{\pi}{\min\{c,p\}}, T^0 + W^0\right\}$, from the third equation of (2.1), we have

$$\frac{dH(\tau)}{d\tau} \leq f + p\alpha\overline{M} - dH(\tau).$$

Therefore for all $\tau \geq 0$,

$$H(\tau) \leq \max\left\{\frac{f + p\alpha\overline{M}}{d}, H^0\right\}.$$

For the last equation of (2.1), we obtain after combining the second and last equations

$$\frac{d}{d\tau}(gD(\tau) + kW(\tau)) \leq ka_1\overline{M}^2 - \min\{p,\nu\}(gD + kW).$$

Therefore,

$$gD(\tau) + kW(\tau) \leq \frac{ka_1\overline{M}^2}{\min\{p,\nu\}} - \left(gD^0 + kW^0 + \frac{ka_1\overline{M}^2}{\min\{p,\nu\}}\right)\exp(-\min\{p,\nu\}\tau)$$

and for all $\tau \geq 0$,

$$gD(\tau) + kW(\tau) \leq \max\left\{\frac{ka_1\overline{M}^2}{\min\{p,\nu\}}, gD^0 + kW^0\right\}.$$

Finally, using the fact that W is bounded, we deduce the boundedness of D. __

The second result of this part deals with the equilibria of (2.1). For a smoother presentation to highlight the impact of dormancy, its reactivation, or the provision of external free viruses on the evolution of the model, we distinguish two cases depending on whether the reactivation of dormant cells (or provision of external free viruses) occurs or not.

Theorem 2. *Let us consider the system* (2.1)*, and define the following quantities and threshold numbers:*

$$b = -a_1 f + cd - a_1\pi\alpha,\ R_0^w = \frac{a_1\pi\alpha}{dc},\ \overline{R_0^w} = 1 + \frac{a_1 p\alpha\nu}{dck} \text{ and } R_1^w = \frac{dck}{a_1 p\alpha\nu}(R_0^w - 1).$$

$$R_w = \frac{a_1\pi k(fk + p\alpha\nu)}{p\nu(a_1 fk + a_1 p\alpha\nu + cdk)}, \qquad \mathcal{T}_w = \frac{-2ka_1 f + k\left(-b + \sqrt{b^2 + 4a_1 cdf}\right)}{2a_1 p\alpha\nu}.$$

1. *Assume $f = 0$. That is, either there is no reactivation of dormant cells, or dormant cells remain dormant forever, or there is no provision of free viruses from external sources. Then, the model has three possible equilibria:*

- *The infection-free equilibrium: IFE $= (\pi/c, 0, 0, 0) = (T^*, 0, 0, 0)$.*
- *If $R_0^w > 1$, we have an immunity-inactivated infection equilibrium given by*

$$EE^1 = (T^1, W^1, H^1, D^1) = \left(\frac{d}{a_1\alpha}; \frac{cd}{p\alpha a_1}(R_0^w - 1); \frac{c}{a_1}(R_0^w - 1); 0\right).$$

- *If $R_0^w > 1 + \frac{a_1 p\alpha\nu}{dck}$ (i.e $R_0^w > \overline{R_0^w}$ or $R_1^w > 1$), we have the immunity-activated infection equilibrium*

$$EE^\sharp = (T^\sharp, W^\sharp, H^\sharp, D^\sharp) = \left(\frac{d\pi k}{a_1 p\alpha\nu + dck};\ \frac{\nu}{k};\ \frac{p\alpha\nu}{dk};\ \frac{a_1 p^2\alpha\nu}{g(a_1 p\alpha\nu + dck)}(R_1^w - 1)\right).$$

2. *Assume $f > 0$. That is, either there is reactivation of dormant cells, or there is provision of free viruses from external sources. Then, the system exhibits the following infection-persistent equilibria.*

- *The unique immunity-inactivated infection equilibrium denoted by*

$\widetilde{EE}^1 = (\widetilde{T}^1, \widetilde{W}^1, \widetilde{H}^1, \widetilde{D}^1)$ *where* $\widetilde{H}^1$ *is the unique positive solution of*

$$a_1 d(\widetilde{H}^1)^2 - (a_1 f - cd + a_1\pi\alpha)\widetilde{H}^1 - cf = 0 \tag{3.3}$$

given by

$$\widetilde{H}^1 = \frac{1}{2a_1 d}\left[-b + \sqrt{b^2 + 4a_1 dcf}\right],$$

and correspondingly,

$$\widetilde{T}^1 = \frac{\pi}{a_1\widetilde{H}^1 + c};\ \widetilde{W}^1 = \frac{a_1\pi\widetilde{H}^1}{p(a_1\widetilde{H}^1 + c)};\ \widetilde{D}^1 = 0.$$

- The unique immunity-activated infection equilibrium, whenever $R_w > 1$, denoted by

$\widetilde{EE}^{\sharp} = (\widetilde{T}^{\sharp}, \widetilde{W}^{\sharp}, \widetilde{H}^{\sharp}, \widetilde{D}^{\sharp})$ *and given by*

$$\widetilde{T}^{\sharp} = \frac{\pi k d}{a_1(kf + p\nu\alpha) + cdk};\ \widetilde{W}^{\sharp} = \frac{\nu}{k};\ \widetilde{H}^{\sharp} = \frac{kf + p\alpha\nu}{kd};\ \widetilde{D}^{\sharp} = \frac{p}{g}(R_w - 1).$$

Proof. The proof of Theorem 2 is straightforward and is not presented here. __

Remark 1. *From the results of Theorem 2, the following interpretations and observations are valid.*

- The threshold parameter $R_0^w = \frac{a_1\pi\alpha}{dc} = a_1\left(\pi\frac{1}{c}\right)\left(\frac{p\alpha}{d}\right)\left(\frac{1}{p}\right)$ denotes the basic reproduction number of infected epithelial cells and its interpretation is as follows: π healthy epithelial cells are generated and infected at a rate a_1 during their lifetime $1/c$ to $p\alpha$ viruses that in turn remain active for $1/d$ and are produced by p infected death epithelial cells during their lifespan of $1/p$ units of time.
- The threshold parameter $R_1^w = \frac{dck}{a_1 p\alpha\nu}(R_0^w - 1)$ can be interpreted as the immune cells' reproduction number. As such, it is a kind of invasive reproduction number of immune cells when infected cells are established (that is, when $R_0^w > 1$).
- Similarly, the threshold parameter $R_w = \frac{a_1\pi k(fk + p\alpha\nu)}{p\nu(a_1 fk + a_1 p\alpha\nu + cdk)}$ is the reproduction number of immune cells when dormant cells reactivate and produce new virus particles.
- In contrast to R_1^w, the threshold R_w is not an invasive reproduction number, because the basic reproduction number of infected cells does not exist in this case. Moreover, the condition $R_1^w \geq 1$ that ensures the existence of the persistent equilibrium can be expressed in the form of $f \geq f_0$, where $f_0 = \frac{a_1 p\alpha\nu(1 - k\pi) + cdk}{a_1 k(k\pi - p\nu)}$ is the minimum rate of reactivation of dormant cells (or provision of external free viruses) necessary to trigger and sustain the immune response. In other words, biologically it means that if dormant cell reactivation is high enough to exceed this minimum threshold value (f_0), then the immune response does not necessarily need to be permanently/consistently active to suppress the infection, and a transient action of the immune response might be enough to serve the purpose.
- The model (2.1) does not admit an infection-free equilibrium if $f > 0$, indicating that a persistent inflow of HPV viral particles within the body will never allow the infected person to eliminate the infection, even in the long run. This may happen when infected individuals maintain unsafe sexual practices or have multiple sexual partners.

4. Local stability and bifurcation analysis

In order to analyse the local stability of the equilibrium points and perform a bifurcation analysis, we apply the linearisation approach and Routh–Hurwitz criteria. The results on the local stability of the equilibria are summarised below.

Theorem 3. *The following local stability results are valid.*

(1) *Assume $f = 0$, then the following statements hold.*

1. *If $R_0^w < 1$, then the infection-free equilibrium IFE is always locally asymptotically stable and unstable otherwise.*
2. *If $1 < R_0^w < 1 + \frac{a_1 p\alpha\nu}{dck}$ (i.e $1 < R_0^w$ and $R_1^w < 1$), then the immunity-inactivated infection equilibrium EE^1, is always locally asymptotically stable and is unstable whenever $R_0^w > 1 + \frac{a_1 p\alpha\nu}{dck}$.*
3. *Assume that $R_0^w > 1 + \frac{a_1 p\alpha\nu}{dck}$ (i.e $R_1^w > 1$), then the immunity-activated infection equilibrium $EE^{\sharp}$ is locally asymptotically stable and may lose its stability whenever $1 + \frac{a_1 p\alpha\nu}{dck}$ exceeds a certain threshold value* (see Fig. 7).

(2) *Assume that $f > 0$, then the following statements hold.*

4. *If $R_w < 1$, the equilibrium of immunity-inactivated infection $\widetilde{EE}^1$ is always locally asymptotically stable and unstable otherwise.*
5. If $R_w > 1$, the equilibrium of immunity-activated infection $\widetilde{EE}^{\sharp}$ exists and is always locally asymptotically stable and unstable otherwise.

Remark 2. The stability of the immunity-activated equilibrium point and the possible loss of stability through the creation of periodic solutions in Theorem 3 highlight the fact that overproduction ($R_1^w > 1$) of immune cells can be detrimental to the human host defence by triggering uncontrollable situations whereby the immune cells can oscillate between favourable and unfavourable outcomes (see Fig. 8(c–d)).

Before the mathematical proof of this result, we first illustrate it with the following bifurcation diagram.

Proof. To perform the proof of Theorem 3, we compute the Jacobian matrix of the right hand side of Model (2.1) given by

$$J(X)=\begin{pmatrix} -a_1H-c & 0 & -a_1T & 0\\ a_1H & -gD-p & a_1T & -gW\\ 0 & p\alpha & -d & 0\\ 0 & kD & 0 & kW-\nu \end{pmatrix}$$

The Jacobian matrix evaluated at *IFE*, gives

$$J(IFE)=\begin{pmatrix} -c & 0 & -a_1\pi/c & 0\\ 0 & -p & a_1\pi/c & 0\\ 0 & p\alpha & -d & 0\\ 0 & 0 & 0 & -\nu \end{pmatrix}$$

Clearly, $J(IFE)$ has two negative eigenvalues $-c$ and $-\nu$ and the remaining eigenvalues are that of the matrix

$$\begin{pmatrix} -p & a_1\pi/c\\ p\alpha & -d \end{pmatrix}$$

whose trace and determinant are $-p-d<0$ and $pd(1-R_0^w)>0$, respectively. Therefore, *IFE* is locally asymptotically stable if $R_0^w<1$.

When evaluated at immunity-inactivated equilibrium EE^1, the characteristic polynomial is

$$(kW^1-\nu-\lambda)[\lambda^3+\lambda^2(a_1H^1+c+p+d)+\lambda(p+d)(a_1H^1+c)+pcd(R_0^w-1)]=0. \tag{4.1}$$

An obvious eigenvalue is $kW^1-\nu=\nu(R_1^w-1)$, which is negative whenever $R_1^w<1$. We use Routh-Hurwitz criteria to determine the signs of the remaining eigenvalues. In this regard, we set

$$q(\lambda)=\lambda^3+A_1\lambda^2+A_2\lambda+A_3 \tag{4.2}$$

where

$$A_1=a_1H^1+c+p+d;\ A_2=(p+d)(a_1H^1+c);\ A_3=pcd(R_0^w-1).$$

We have $A_i>0$; $i=1,2,3$ since $R_0^w>1$.

$$\begin{aligned} A_1A_2-A_3 &= (a_1H_i^1+c+p+d)(p+d)(a_1H^1+c)-pcd(R_0^w-1)\\ &= cR_0^w(p+d)(cR_0^w+p+d)-pcd(R_0^w-1)\\ &= (cpR_0^w+cdR_0^w)(cR_0^w+p+d)-pcdR_0^w+pcd\\ &= cpR_0^w(cR_0^w+p)+pcd+cdR_0^w(cR_0^w+p+d)>0; \end{aligned}$$

Therefore, EE^1 is always locally asymptotically stable.

The evaluation of the Jacobian matrix $J(X)$ at $EE^\sharp$, gives the characteristic polynomial

$$\lambda^4+B_1\lambda^3+B_2\lambda^2+B_3\lambda+B_4=0. \tag{4.3}$$

The coefficients B_1, B_2, B_3, B_4 can be seen as functions of k and lengthy calculations lead to

$$\begin{aligned} B_1(k) &= gD^\sharp+p+d+a_1H^\sharp+c>0,\\ B_2(k) &= gdD^\sharp+g\nu D^\sharp+pd-a_1T^\sharp p\alpha+(a_1H^\sharp+c)(gD^\sharp+p+d),\\ &= g\nu D^\sharp+(a_1H^\sharp+c)(gD^\sharp+p+d)>0 \end{aligned}$$

$$\begin{aligned} B_3(k) &= g\nu dD^\sharp+(a_1H^\sharp+c)(gdD^\sharp+g\nu D^\sharp+pd-a_1T^\sharp p\alpha)+a_1^2T^\sharp H^\sharp p\alpha\\ &= a_1^2T^\sharp H^\sharp p\alpha+g\nu dD^\sharp+g\nu D^\sharp(a_1H^\sharp+c)>0\\ B_4(k) &= \nu gdD^\sharp(a_1H^\sharp+c)>0. \end{aligned}$$

$$\begin{aligned}B_1(k)B_2(k)-B_3(k)&=(gD^\sharp+p+d+a_1H^\sharp+c)[g\nu D^\sharp+(a_1H^\sharp+c)(gD^\sharp+p+d)]-[a_1^2T^\sharp H^\sharp p\alpha+g\nu dD^\sharp+g\nu D^\sharp(a_1H^\sharp+c)]\\&=(gD^\sharp+p)[g\nu D^\sharp+(a_1H^\sharp+c)(gD^\sharp+p+d)]+cd(gD^\sharp+p+d)+a_1dgH^\sharp D^\sharp\\&+a_1d^2H^\sharp+(a_1H^\sharp+c)^2(gD^\sharp+p+d)-a_1dgH^\sharp D^\sharp\\&=(gD^\sharp+p)[g\nu D^\sharp+(a_1H^\sharp+c)(gD^\sharp+p+d)]+cd(gD^\sharp+p+d)+a_1d^2H^\sharp+(a_1H^\sharp+c)^2(gD^\sharp+p+d)>0.\end{aligned}$$

When applying the Routh-Hurwitz criteria to establish the local asymptotic stability of the equilibrium point $EE^\sharp$, it remains to find the conditions under which the quantity $\varphi(k)$ given below is positive.

$$\varphi(k)=(B_1(k)B_2(k)-B_3(k))B_3(k)-B_1^2(k)B_4(k). \tag{4.4}$$

Straightforward, but lengthy computations lead to

$$\begin{aligned}\varphi(k)&=[a_1^2T^\sharp H^\sharp p\alpha+g\nu dD^\sharp+g\nu D^\sharp(a_1H^\sharp+c)]\times\\&[(gD^\sharp+p)[g\nu D^\sharp+(a_1H^\sharp+c)(gD^\sharp+p+d)]+cd(gD^\sharp+p+d)+a_1d^2H^\sharp+(a_1H^\sharp+c)^2(gD^\sharp+p+d)]-\\&\nu gdD^\sharp(a_1H^\sharp+c)[gD^\sharp+p+d+a_1H^\sharp+c]^2\end{aligned}$$

$$\begin{aligned}\varphi(k)&=(a_1^2T^\sharp H^\sharp p\alpha+g\nu dD^\sharp)\times\\&[(gD^\sharp+p)[g\nu D^\sharp+(a_1H^\sharp+c)(gD^\sharp+p+d)]+cd(gD^\sharp+p+d)+a_1d^2H^\sharp+(a_1H^\sharp+c)^2(gD^\sharp+p+d)]+\\&g\nu D^\sharp(a_1H^\sharp+c)[(gD^\sharp+p)[g\nu D^\sharp+(a_1H^\sharp+c)(gD^\sharp+p+d)]+cd(gD^\sharp+p+d)+a_1d^2H^\sharp]+\\&g\nu D^\sharp(a_1H^\sharp+c)^3(gD^\sharp+p+d)-\\&\nu gdD^\sharp(a_1H^\sharp+c)^3-2\nu gdD^\sharp(a_1H^\sharp+c)^2(gD^\sharp+p+d)-\nu gdD^\sharp(a_1H^\sharp+c)(gD^\sharp+p+d)^2\end{aligned}$$

After lengthy and tedious calculations using the model's equilibrium equations, we succeeded in putting $\varphi(k)$ into the following reduced form.

$$\begin{aligned}\varphi(k)&=a_ip^2\alpha W^\sharp(gD^\sharp+p)[(a_1H^\sharp+c)(gD^\sharp+p+d)]+(gD^\sharp+p+d)(cd+(a_1H^\sharp+c)^2)+a_1d^2H^\sharp\Big)\\&+a_1p\alpha gD^\sharp W^\sharp(gD^\sharp+p)[a_1H^\sharp(gD^\sharp+p+d)+c(gD^\sharp+p)])\\&+a_1p\alpha gD^\sharp W^\sharp\Big((gD^\sharp+p+d)(cd+(a_1H^\sharp+c)^2)+a_1d^2H^\sharp\Big)\\&+a_1gdD^\sharp(gD^\sharp+p)\Big(cp\alpha W^\sharp+ca_1\nu H^\sharp+\nu pH^\sharp+\nu c^2+g\nu D^\sharp\Big/a_1+p\alpha\nu gD^\sharp W^\sharp\Big/d-\nu p\alpha W^\sharp\Big)+\\&g\nu D^\sharp(a_1H^\sharp+c)[(gD^\sharp+p)(g\nu D^\sharp+(a_1H^\sharp+c)(gD^\sharp+p))]+g\nu D^\sharp(a_1H^\sharp+c)^3(gD^\sharp+p).\end{aligned}$$

This computation shows that the function $\varphi(k)$ can change the sign, depending on the chosen set of parameters. For instance, if one has a set of model parameters, such that $R_0^w>1+\frac{a_1p\alpha\nu}{dck}$, and

$$cp\alpha W^\sharp+ca_1\nu H^\sharp+\nu pH^\sharp+\nu c^2+g\nu D^\sharp\Big/a_1+p\alpha\nu gD^\sharp W^\sharp\Big/d-\nu p\alpha W^\sharp\geq 0,$$

then the equilibrium point $EE^\sharp$ is locally asymptotically stable. This local stability condition holds for many instances, for example, when $R_0^w>\overline{R_0^w}$ and $c>p$, or whenever $R_0^w>\overline{R_0^w}>\frac{\nu p\alpha}{(ck)^2}$. On the other hand, when there exists a set of model parameters (or equivalently, some k) such that $\varphi(k)<0$, then the equilibrium $EE^\sharp$ loses its stability. The Hopf bifurcation that emerges from this loss of local stability will be established and numerically illustrated shortly.

The characteristic polynomial of Model (2.1) at $\widetilde{EE}^1$ gives

$$(k\widetilde{W}^1-\nu-\lambda)(\lambda^3+M_1\lambda^3+M_2\lambda^2+M_3)=0, \tag{4.5}$$

where the coefficients M_1, M_2, M_3 are given by:

$$
\begin{aligned}
M_1 &= a_1\widetilde{H}^1 + c + p + d > 0\\
M_2 &= (p+d)(a_1\widetilde{H}^1 + c) + pd - a_1 p\alpha\widetilde{T}^1\\
&= (p+d)(a_1\widetilde{H}^1 + c) + \frac{p(d\widetilde{H}^1 - p\alpha\widetilde{W}^1)}{\widetilde{H}^1}\\
&= (p+d)(a_1\widetilde{H}^1 + c) + \frac{pf}{\widetilde{H}^1} > 0\\
M_3 &= (a_1\widetilde{H}^1 + c)(pd - a_1 p\alpha\widetilde{T}^1) + a_1^2 p\alpha\widetilde{T}^1\widetilde{H}^1\\
&= \frac{pf}{\widetilde{H}^1}(a_1\widetilde{H}^1 + c) + a_1^2 p\alpha\widetilde{T}^1\widetilde{H}^1 > 0\\
M_1M_2 - M_3 &= \left[a_1\widetilde{H}^1 + c + p + d\right]\left[(p+d)(a_1\widetilde{H}^1 + c) + \frac{pf}{\widetilde{H}^1}\right] - \left[\frac{pf}{\widetilde{H}^1}(a_1\widetilde{H}^1 + c) + a_1^2 p\alpha\widetilde{T}^1\widetilde{H}^1\right]\\
&= \frac{pf(p+d)}{\widetilde{H}^1} + a_1 pf + a_1 p\widetilde{H}^1(a_1\widetilde{H}^1 + c + p) + (a_1\widetilde{H}^1 + c + p + d)(pc + d(a_1\widetilde{H}^1 + c)) > 0
\end{aligned}
$$

Since $k\widetilde{W}^1 - \nu = \nu(\mathcal{T}_w - 1) < 0$ if $\mathcal{T}_w < 1$, we use the Routh-Hurwitz criteria to conclude that the equilibrium point $\widetilde{EE}^1$ is locally asymptotically stable.

Computing the characteristic polynomial of the Jacobian matrix of Model (2.1) at $\widetilde{EE}^\sharp$, we obtain

$$\lambda^4 + C_1\lambda^3 + C_2\lambda^2 + C_3\lambda + C_4 = 0, \tag{4.6}$$

where the coefficients C_1, C_2, C_3, C_4 are given as below.

$$
\begin{aligned}
C_1 &= a_1\widetilde{H}^\sharp + c + g\widetilde{D}^\sharp + p + d > 0,\\
C_2 &= (a_1\widetilde{H}^\sharp + c)(g\widetilde{D}^\sharp + p + d) + gk\widetilde{D}^\sharp\widetilde{W}^\sharp + gd\widetilde{D}^\sharp + pd - a_1\widetilde{T}^\sharp p\alpha,\\
&= (a_1\widetilde{H}^\sharp + c)(g\widetilde{D}^\sharp + p + d) + gk\widetilde{D}^\sharp\widetilde{W}^\sharp + \frac{gd\widetilde{D}^\sharp\widetilde{H}^\sharp + pd\widetilde{H}^\sharp - a_1\widetilde{T}^\sharp\widetilde{H}^\sharp p\alpha}{\widetilde{H}^\sharp}\\
&= (a_1\widetilde{H}^\sharp + c)(g\widetilde{D}^\sharp + p + d) + gk\widetilde{D}^\sharp\widetilde{W}^\sharp + \frac{gd\widetilde{D}^\sharp\widetilde{H}_i^\sharp + p_i^2\alpha\widetilde{W}^\sharp - a_1\widetilde{T}^\sharp\widetilde{H}^\sharp p\alpha + pf}{\widetilde{H}^\sharp}\\
&= (a_1\widetilde{H}^\sharp + c)(g\widetilde{D}^\sharp + p + d) + gk\widetilde{D}^\sharp\widetilde{W}^\sharp + \frac{g\widetilde{D}^\sharp(d\widetilde{H}^\sharp - p\alpha\widetilde{W}^\sharp) + pf}{\widetilde{H}^\sharp}\\
&= (a_1\widetilde{H}^\sharp + c)(g\widetilde{D}^\sharp + p + d) + gk\widetilde{D}^\sharp\widetilde{W}^\sharp + \frac{f(g\widetilde{D}^\sharp + p)}{\widetilde{H}^\sharp} > 0\\
C_3 &= a_1^2 p\alpha\widetilde{T}^\sharp\widetilde{H}^\sharp + gdk\widetilde{D}^\sharp\widetilde{W}^\sharp + (a_1\widetilde{H}^\sharp + c)[gk\widetilde{D}^\sharp\widetilde{W}^\sharp + gd\widetilde{D}^\sharp + pd - a_1\widetilde{T}^\sharp p\alpha]\\
&= a_1^2 p\alpha\widetilde{T}^\sharp\widetilde{H}^\sharp + gdk\widetilde{D}^\sharp\widetilde{W}^\sharp + (a_1\widetilde{H}^\sharp + c)\left[gk\widetilde{D}^\sharp\widetilde{W}^\sharp + \frac{f(g\widetilde{D}^\sharp + p)}{\widetilde{H}^\sharp}\right] > 0\\
C_4 &= gdk\widetilde{D}^\sharp\widetilde{W}^\sharp(a_1\widetilde{H}^\sharp + c) > 0.\\
C_1C_2 - C_3 &= (a_1\widetilde{H}^\sharp + c)^2(g\widetilde{D}^\sharp + p + d) + a_1 f(g\widetilde{D}^\sharp + p) +\\
&\quad (g\widetilde{D}^\sharp + p)\left[cd + (a_1\widetilde{H}^\sharp + c)(g\widetilde{D}^\sharp + p) + gk\widetilde{D}^\sharp\widetilde{W}^\sharp + \frac{f(g\widetilde{D}^\sharp + p)}{\widetilde{H}^\sharp}\right] +\\
&\quad d\left[(a_1\widetilde{H}^\sharp + c)(g\widetilde{D}^\sharp + p + d) + \frac{f(g\widetilde{D}^\sharp + p)}{\widetilde{H}^\sharp}\right] > 0
\end{aligned}
$$

$$(C_1C_2 - C_3)C_3 - C_1^2C_4 = a_1^2p\alpha\widetilde{T}^\sharp\widetilde{H}^\sharp\Big[(a_1\widetilde{H}^\sharp + c)^2(g\widetilde{D}^\sharp + p + d) + a_1f(g\widetilde{D}^\sharp + p)\Big] +$$

$$a_1^2p\alpha\widetilde{T}^\sharp\widetilde{H}^\sharp\left[(g\widetilde{D}^\sharp + p)\left[cd + (a_1\widetilde{H}^\sharp + c)(g\widetilde{D}^\sharp + p) + gk\widetilde{D}^\sharp\widetilde{W}^\sharp + \frac{f(g\widetilde{D}^\sharp + p)}{\widetilde{H}^\sharp}\right]\right] +$$

$$a_1^2p\alpha d\widetilde{T}^\sharp\widetilde{H}^\sharp\left[(a_1\widetilde{H}^\sharp + c)(g\widetilde{D}^\sharp + p + d) + \frac{f(g\widetilde{D}^\sharp + p)}{\widetilde{H}^\sharp}\right] +$$

$$\frac{f(a_1\widetilde{H}^\sharp + c)(g\widetilde{D}^\sharp + p)}{\widetilde{H}^\sharp}\Big[(a_1\widetilde{H}^\sharp + c)^2(g\widetilde{D}^\sharp + p + d) + a_1f(g\widetilde{D}^\sharp + p)\Big] +$$

$$\frac{f(a_1\widetilde{H}^\sharp + c)(g\widetilde{D}^\sharp + p)^2}{\widetilde{H}^\sharp}\left[cd + (a_1\widetilde{H}^\sharp + c)(g\widetilde{D}^\sharp + p) + gk\widetilde{D}^\sharp\widetilde{W}^\sharp + \frac{f(g\widetilde{D}^\sharp + p)}{\widetilde{H}^\sharp}\right] +$$

$$\frac{df(a_1\widetilde{H}^\sharp + c)(g\widetilde{D}^\sharp + p)}{\widetilde{H}^\sharp}\left[(a_1\widetilde{H}^\sharp + c)(g\widetilde{D}^\sharp + p + d) + \frac{f(g\widetilde{D}^\sharp + p)}{\widetilde{H}^\sharp}\right] +$$

$$cgk\widetilde{D}^\sharp\widetilde{W}^\sharp\left[(a_1\widetilde{H}^\sharp + c)^2(g\widetilde{D}^\sharp + p) + a_1f(g\widetilde{D}^\sharp + p) + \frac{df(g\widetilde{D}^\sharp + p)}{\widetilde{H}^\sharp}\right] +$$

$$cgk\widetilde{D}^\sharp\widetilde{W}^\sharp\left[(g\widetilde{D}^\sharp + p)\left(cd + (a_1\widetilde{H}^\sharp + c)(g\widetilde{D}^\sharp + p) + gk\widetilde{D}^\sharp\widetilde{W}^\sharp + \frac{f(g\widetilde{D}^\sharp + p)}{\widetilde{H}^\sharp}\right)\right] +$$

$$a_1gk\widetilde{D}^\sharp\widetilde{W}^\sharp\widetilde{H}^\sharp\Big[(a_1\widetilde{H}^\sharp + c)^2(g\widetilde{D}^\sharp + p) + a_1f(g\widetilde{D}^\sharp + p)\Big] +$$

$$a_1gk\widetilde{D}^\sharp\widetilde{W}^\sharp\widetilde{H}^\sharp\left[(g\widetilde{D}^\sharp + p)\left(cd + (a_1\widetilde{H}^\sharp + c)(g\widetilde{D}^\sharp + p) + gk\widetilde{D}^\sharp\widetilde{W}^\sharp + \frac{f(g\widetilde{D}^\sharp + p)}{\widetilde{H}^\sharp}\right)\right] +$$

$$gkd\widetilde{D}^\sharp\widetilde{W}^\sharp\left[(g\widetilde{D}^\sharp + p)\left(gk\widetilde{D}^\sharp\widetilde{W}^\sharp + \frac{f(g\widetilde{D}^\sharp + p)}{\widetilde{H}^\sharp}\right) + \frac{f(g\widetilde{D}^\sharp + p)}{\widetilde{H}^\sharp}\right] +$$

$$\frac{a_1gf^2k\widetilde{D}^\sharp\widetilde{W}^\sharp(g\widetilde{D}^\sharp + p)}{\widetilde{H}^\sharp} + a_1gdfk\widetilde{D}^\sharp\widetilde{W}^\sharp(g\widetilde{D}^\sharp + p)\left[2 - \frac{d\widetilde{H}^\sharp}{f} - \frac{f}{d\widetilde{H}^\sharp}\right] > 0$$

Remark 3. The long-term behaviour of the model (2.1) established in Theorem 3 hereby validate the definitions of the threshold parameters R_1^w and R_w. In fact, the threshold R_1^w *(*resp. R_w*)* measures the proliferation potential of immune cells in the absence *(*resp. in the presence*)* of dormant cells reactivation.

The local asymptotic stability of the equilibria proved in Theorem 3 suggests the possibility of trans-critical bifurcations at $R_0^w = 1$; $R_0^w = 1 + \frac{a_1p\alpha\nu}{dck}$ and $R_w = 1$; and a Hopf bifurcation around the immunity-activated equilibrium $EE^\sharp$, as one can see in the following result.

Theorem 4. *The system model* (2.1) *exhibits three trans-critical forward bifurcations: one at the infection-free equilibrium IFE when* $R_0^w = 1$, *the second at the immunity-inactivated equilibrium* EE^1 *when* $R_0^w = 1 + \frac{a_1p\alpha\nu}{dck}$, *and the last one at the immunity-inactivated equilibrium* $\widetilde{EE}^1$ *when* $R_w = 1$. *More remarkably, the immunity-activated equilibrium* $EE^\sharp$ *of the model* (2.1) *can lose its stability through a Hopf bifurcation.*

Proof. We begin by investigating the occurrence of a Hopf bifurcation. Assuming that (4.3) has a pair of pure imaginary solutions $\pm\sigma i$, with $\sigma > 0$, we have, after replacing λ by σi in (4.3)

$$\sigma = \sqrt{B_3/B_1} \text{ with } B_1 > 0, B_4 > 0, B_1B_2 - B_3 > 0, (B_1B_2 - B_3)B_3 - B_1^2B_4 = 0.$$

We choose k as a bifurcation parameter and recall the function $\varphi(k)$ in Equation (4.4) above.

Assuming that there exists a k^* >0 such that

$$B_1(k^*) > 0, B_4(k^*) > 0, B_1(k^*)B_2(k^*) - B_3(k^*) > 0, \varphi(k^*) = 0.$$

Then (4.3) has four roots: $\pm\sigma i$, λ_1 and λ_2 where $\sigma = \pm\sqrt{B_3(k^*)/B_1(k^*)}$, $\mathrm{Re}(\lambda_1) < 0$ and $\mathrm{Re}(\lambda_2) < 0$. When $0 < |k - k^*| \ll 1$, we assume that (4.3) has four roots: $\alpha(k) \pm i\sigma(k)$, $\lambda_1(k)$ and $\lambda_2(k)$. In what follows, we determine the derivative of $\alpha(k)$ and evaluate it at k^*. We know that

$$(\alpha(k) + i\sigma(k))^4 + B_1(\alpha(k) + i\sigma(k))^3 + B_2(\alpha(k) + i\sigma(k))^2 + B_3(\alpha(k) + i\sigma(k)) + B_4 = 0. \tag{4.7}$$

Taking the derivative of (4.7) with respect to k, we obtain:

$$\begin{aligned}&\alpha'(k) + i\sigma'(k))[4(\alpha(k) + i\sigma(k))^3 + 3B_1(k_1)(\alpha(k) + i\sigma(k))^2 + 2B_2(k)(\alpha(k) + i\sigma(k)) + B_3]+\\ &B_1'(k)(\alpha(k) + i\sigma(k))^3 + B_2'(k)(\alpha(k) + i\sigma(k))^2 + B_3'(k)(\alpha(k) + i\sigma(k)) + B_4'(k) = 0.\end{aligned}$$

After reducing calculations, we obtain

$$((\alpha'(k) + i\sigma'(k)))(A(k) + iB(k)) + C(k) + iD(k) = 0 \tag{4.8}$$

where,

$$\begin{aligned}A(k) &= 4\alpha^3(k) - 12\alpha(k)\sigma^2(k) + 3B_1(k)\alpha^2(k) - 3B_1(k)\sigma^2(k) + 2B_2(k)\alpha(k) + B_3(k);\\ B(k) &= 12\alpha^2(k)\sigma(k) - 4\sigma^3(k) + 6B_1(k)\alpha(k)\sigma(k) + 2B_2(k)\sigma(k);\\ C(k) &= B_1'(k)\alpha^3(k) - 3B_1'(k)\alpha(k)\sigma^2(k) + B_2'(k)\alpha^2(k) - B_2'(k)\sigma^2(k) + B_3'(k)\alpha(k) + B_4'(k);\\ D(k) &= 3B_1'(k)\alpha^2(k)\sigma(k) - B_1'(k)\sigma^3(k) + 2B_2'(k)\alpha(k)\sigma + B_3'(k)\sigma(k).\end{aligned}$$

By separating the real and imaginary parts, equation (4.8) takes the following form

$$\begin{pmatrix} A(k) & -B(k) \\ B(k) & A(k) \end{pmatrix}\begin{pmatrix} \alpha'(k) \\ \sigma'(k) \end{pmatrix} + \begin{pmatrix} C(k) \\ D(k) \end{pmatrix} = \begin{pmatrix} 0 \\ 0 \end{pmatrix},$$

whose unique solution is given by

$$\alpha'(k) = -\frac{A(k)C(k) + B(k)D(k)}{A^2(k) + B^2(k)}.$$

Evaluating $\alpha'(k)$ at k^* and using $\varphi(k^*) = 0$, we obtain after calculations:

$$\alpha'(k_i^*) = -\frac{B_1(k^*)}{2[(B_1(k)B_2(k) - 2B_3(k))^2 + B_3(k)B_1^3(k)]}\varphi'(k_i^*).$$

Therefore, if there exists $k^* > 0$ (to be checked numerically) such that $B_1(k^*) > 0$, $B_4(k^*) > 0$, $B_1(k^*)B_2(k^*) - B_3(k^*) > 0$ and $\varphi'(k^*) \neq 0$, then Model (2.1) exhibits a Hopf bifurcation around the equilibrium point $EE^\sharp$.

For the analysis of the bifurcation at the infection-free equilibrium, we use the approach from Castillo-Chavez, Theorem 4.1 (Zhang et al., 2025) with similar notations. To this end, we recall the Jacobian matrix computed at the infection-free equilibrium given by:

$$J(IFE) = \begin{pmatrix} -c & 0 & -a_1\pi/c & 0 \\ 0 & -p & a_1\pi/c & 0 \\ 0 & p\alpha & -d & 0 \\ 0 & 0 & 0 & -\nu \end{pmatrix}$$

On the other hand, we choose α as the bifurcation parameter. When $\alpha = \alpha^* = \frac{cd}{a_1\pi}$ obtained by solving for α the equation $R_0^w = 1$, we have

$$J(IFE)|_{\alpha=\alpha^*} = \begin{pmatrix} -c & 0 & -a_1\pi/c & 0 \\ 0 & -p & a_1\pi/c & 0 \\ 0 & p\alpha^* & -d & 0 \\ 0 & 0 & 0 & -\nu \end{pmatrix}$$

Obviously, the matrix $J(IFE)|_{\alpha=\alpha^*}$ has only one simple zero eigenvalue and three other eigenvalues with negative real parts. The associated left eigenvector $v = (v_1, v_2, v_3, v_4)$ and right eigenvector $w = (w_1, w_2, w_3, w_4)$ corresponding to the zero eigenvalue are given by $v_1 = v_4 = 0$; $v_2 = \alpha^* v_3$, $v_3 > 0$, and $w_1 = -\frac{a_1\pi}{c^2}w_3, w_1 = \frac{a_1\pi}{cp}w_3, w_4 = 0, w_3 > 0$.

After lengthy calculations, we obtain the following for a and b:

$$a = -2a_1^2\frac{\alpha^*\pi v_3 w_3^2}{c^2} < 0;\ b = \frac{a_1\pi v_3 w_3}{c} > 0.$$

Therefore, Model (2.1) presents a forward bifurcation at the infection-free equilibrium *IFE* whenever $\alpha = \alpha^*$ (that is, $R_0^w = 1$).

A similar reasoning and notations for the immunity-inactivated equilibrium lead to the following:

We recall the Jacobian matrix computed at this equilibrium

$$J(EE^1)|_{k=k^*} = \begin{pmatrix} -cR_0^w & 0 & -d/\alpha & 0 \\ c(R_0^w - 1) & -p & d/\alpha & -gcd(R_0^w - 1)/a_1 p\alpha \\ 0 & p\alpha & -d & 0 \\ 0 & 0 & 0 & 0 \end{pmatrix},$$

where k is a bifurcation parameter and $k^* = \frac{a_1 p\alpha\nu}{cd(R_0^w - 1)}$ is obtained by solving for k the equation $R_1^w = 1$.

For the simple zero eigenvalue of $J(EE^1)|_{k=k^*}$, the associated left eigenvector $v = (v_1, v_2, v_3, v_4)$ and right eigenvector $w = (w_1, w_2, w_3, w_4)$ are given by $v_1 = v_2 = v_3 = 0$; $v_4 > 0$, and $w_1 = \frac{gd}{a_1 p\alpha}w_4, w_2 = -\frac{gcdR_0^w}{a_1 p^2\alpha}w_4, w_3 = -\frac{gcR_0^w}{a_1 p}w_4$ and $w_4 > 0$.

After lengthy calculations, we obtain the following for a and b:

$$a = -\frac{2k^* gcdR_0^w}{a_1 p^2\alpha}v_4 w_4^2 < 0;\ b = \frac{cd(R_0^w - 1)}{a_1 p\alpha}v_4 w_4 > 0.$$

Therefore a forward bifurcation around the immunity-inactivated equilibrium EE^1 (whenever it exists) of model (2.1) occurs at $k = k^*$, corresponding to $R_1^w = 1$.

For the immunity-inactivated equilibrium $\widetilde{EE}^1$, we have

$$J(\widetilde{EE}^1)|_{k=k^*} = \begin{pmatrix} -a_1\widetilde{H}^1 - c & 0 & -a_1\widetilde{T}^1 & 0 \\ a_1\widetilde{H}^1 & -p & a_1\widetilde{T}^1 & -g\widetilde{W}^1 \\ 0 & p\alpha & -d & 0 \\ 0 & 0 & 0 & 0 \end{pmatrix}$$

where k^* is the unique positive solution of the equation

$$a_1\pi f k^2 + k(a_1\pi p\alpha\nu - a_1 fp\nu - cdp\nu) - a_1\alpha p^2\nu = 0 \tag{4.9}$$

obtained by solving $R_w = 1$, given by

$$k^* = \frac{1}{2a_1\pi f}\left(-(a_1\pi p\alpha\nu - a_1 fp\nu - cdp\nu) + \sqrt{(a_1\pi p\alpha\nu - a_1 fp\nu - cdp\nu)^2 + 4a_1^2\pi f\alpha p^2\nu}\right). \tag{4.10}$$

For the simple zero eigenvalue of $J(\widetilde{EE}^1)|_{k=k^*}$, the associated left eigenvector $v = (v_1, v_2, v_3, v_4)$ and right eigenvector $w = (w_1, w_2, w_3, w_4)$ are given by $v_1 = v_2 = v_3 = 0$, $v_4 > 0$, $w_4 > 0$ and

$$w_1 = -\frac{a_1 g\alpha\widetilde{T}^1\widetilde{W}^1}{a_1 c\alpha\widetilde{T}^1 - d(a_1\widetilde{H}^1 + c)}w_4, w_2 = \frac{gd\widetilde{W}^1(a_1\widetilde{H}^1 + c)}{p(a_1 c\alpha\widetilde{T}^1 - d(a_1\widetilde{H}^1 + c))}w_4, w_3 = \frac{g\alpha\widetilde{W}^1(a_1\widetilde{H}^1 + c)}{a_1 c\alpha\widetilde{T}^1 - d(a_1\widetilde{H}^1 + c)}w_4.$$

After lengthy calculations, we obtain the following for a and b:

$$a = \frac{gd\widetilde{W}^1(a_1\widetilde{H}^1 + c)}{p(a_1 c\alpha\widetilde{T}^1 - d(a_1\widetilde{H}^1 + c))}v_4 w_4^2;\ b = \widetilde{W}^1 v_4 w_4 > 0.$$

Note that

$$
\begin{aligned}
a_1 c\alpha\widetilde{T}^1 - d(a_1\widetilde{H}^1 + c) &= \frac{a_1 c\alpha\widetilde{T}^1\widetilde{H}^1 - d\widetilde{H}^1(a_1\widetilde{H}^1 + c)\Big)}{\widetilde{H}^1} \\
&= \frac{c\alpha p\widetilde{W}^1 - d\widetilde{H}^1(a_1\widetilde{H}^1 + c)\Big)}{\widetilde{H}^1} \\
&= \frac{c(d\widetilde{H}^1 - f) - d\widetilde{H}^1(a_1\widetilde{H}^1 + c)\Big)}{\widetilde{H}^1} \\
&= \frac{-cf - a_1 d(\widetilde{H}^1)^2}{\widetilde{H}^1} < 0.
\end{aligned}
$$

Then $a < 0$ and the existence of the forward bifurcation around the immunity-inactivated immune equilibrium $\widetilde{EE}^1$ occurs at $k = k^*$ (given by (4.10)) is proved. The two transcritical bifurcations are illustrated in Fig. 2.

5. Global stability analysis

We combine Lyapunov's and LaSalle's techniques to prove the global asymptotic stability of all equilibria, except that of the immunity-activated equilibrium, in the case without the provision of free viruses. We summarise our results in the following theorem. Before proceeding, we state an instrumental result which proves that $\mathcal{T}_w$ and R_w are equivalent thresholds in the epidemiological sense.

Lemma 1. *The threshold parameters $\mathcal{T}_w$ and R_w are epidemiologically equivalent in the sense that they verify the following equivalence:*

$$\mathcal{T}_w \leq 1 \Leftrightarrow R_w \leq 1.$$

Proof. We have

$$
\begin{aligned}
\mathcal{T}_w \leq 1 \quad &\Leftrightarrow \quad -2ka_1 f + k\left(-b + \sqrt{b^2 + 4a_1 cdf}\right) \leq 2a_1 p\alpha\nu \\
&\Leftrightarrow \quad k\sqrt{b^2 + 4a_1 cdf} \leq 2ka_1 f + kb + 2a_1 p\alpha\nu \\
&\Leftrightarrow \quad k^2(a_1 f - cd + a_1\pi\alpha)^2 + 4k^2 a_1 cdf \leq k^2(a_1 f + cd - a_1\pi\alpha)^2 + \\
&\quad\ 4ka_1 p\alpha\nu(a_1 f + cd - a_1\pi\alpha) + 4(a_1 p\alpha\nu)^2 \\
&\Leftrightarrow \quad 4k^2 a_1^2 f\pi\alpha \leq 4ka_1^2 p\alpha\nu f + 4ka_1 p\alpha\nu cd + 4(a_1 p\alpha\nu)^2 \\
&\Leftrightarrow \quad k^2 a_1^2 f\pi\alpha + ka_1^2 p\alpha^2\nu\pi \leq ka_1^2 p\alpha\nu f + ka_1 p\alpha\nu cd + (a_1 p\alpha\nu)^2 \\
&\Leftrightarrow \quad ka_1^2\pi\alpha(kf + p\alpha\nu) \leq \alpha a_1 p\nu(a_1 kf + kcd + a_1 p\alpha\nu) \\
&\Leftrightarrow \quad ka_1\pi(kf + p\alpha\nu) \leq p\nu(a_1 kf + kcd + a_1 p\alpha\nu) \\
&\Leftrightarrow \quad R_w \leq 1.
\end{aligned}
$$

Theorem 5. *The following results are valid.*

When $f = 0$, then.

1. *If $R_0^w \leq 1$, the infection-free equilibrium IFE is globally asymptotically stable in $\mathbb{R}^4_+$, and otherwise unstable.*
2. *If $1 < R_0^w \leq 1 + \frac{a_1 p\alpha\nu}{dck}$ the equilibrium of immunity-inactivated infection EE^1 is globally asymptotically stable in $\mathbb{R}^4_+ \setminus \{IFE\}$ and unstable when $R_0^w > 1 + \frac{a_1 p\alpha\nu}{dck} = \overline{R_0^w}$.*

On the other hand, when $f > 0$, then.

3. *If $R_w \leq 1$, $\left(\text{or equivalently } 0 < f \leq \frac{p\nu(a_1\alpha p\nu + cdk - a_1\pi\alpha k)}{a_1 k(\pi k - a_1 p\nu)}\right)$ the immunity-inactivated infection equilibrium $\widetilde{EE}^1$ is globally asymptotically stable in $\mathbb{R}^4_+$ and unstable otherwise.*

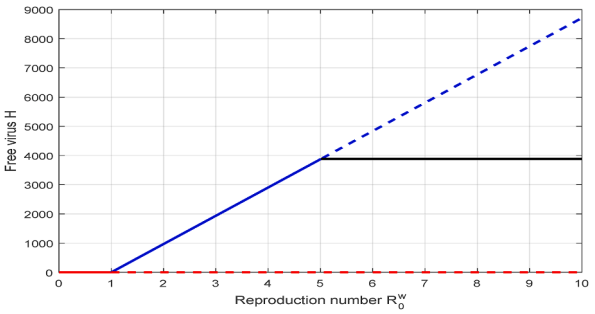

Fig. 2. Bifurcation diagram of model. Two transcritical bifurcations occur at $R_0^w = 1$ and at $R_0^w = 1 + \frac{a_1 p\alpha\nu}{dck} = 5$. When $0 \le R_0^w \le 1$, (red continuous line) the infection-free equilibrium exists and is GAS; When $1 < R_0^w < 5$, *IFE* loses its stability in favour of EE^1, which is also GAS (blue continuous line). Here, the infection occurs, but the immune response is still inactive. When $5 < R_0^w$, EE^1 becomes unstable and $EE^\sharp$ occurs and is LAS (black continuous line) and can undergo Hopf bifurcation; here, the immune response is activated in order to clear the infection. Dotted lines correspond to the unstable states (red color for *IFE*) and (blue color for EE^1.).

4. *Assume* $R_w > 1$, *(or equivalently* $f > \frac{p\nu(a_1\alpha p\nu + cdk - a_1\pi\alpha k)}{a_1 k(\pi k - a_1 p\nu)}$*) then the equilibrium of immunity-activated infection* $\widetilde{EE}^\sharp$ *is globally asymptotically stable in* $\mathbb{R}^4_+ \setminus \{\widetilde{EE}^1\}$ *and otherwise unstable.*

Proof.

1. Let us define the following Lyapunov candidate:

$$L_0 = \left(T - T^* - T^* \ln \frac{T}{T^*}\right) + W + \frac{1}{\alpha} H.$$

Its time derivative along the positive solution of (2.1) gives

$$\frac{dL_0}{d\tau} = -\frac{c}{T}(T - T^*)^2 + \frac{d}{\alpha} H(R_0^w - 1) - gDW.$$

Therefore, under the assumption $R_0^w \le 1$, we have $dL_0/d\tau \le 0$, additionally, $T = T^*$, $W = 0$, $H = 0$, $D = 0$ when $dL_0/d\tau = 0$. Moreover, the singleton (T^*, 0, 0, 0) is the largest compact invariant set in $\{(T, W, H, D) \in \mathbb{R}^4_+;\ dL_0/d\tau = 0\}$. By applying LaSalle's invariance principle, the infection-free equilibrium *IFE* is globally asymptotically stable and unstable whenever $R_0^w > 1$.

2. In order to prove the global asymptotic stability of EE^1, we consider the following Lyapunov candidate:

$$L_1 = \left(T - T^1 - T^1 \ln \frac{T}{T^1}\right) + \left(W - W^1 - W^1 \ln \frac{W}{W^1}\right) + \frac{1}{\alpha}\left(H - H^1 - H^1 \ln \frac{H}{H^1}\right) + \frac{g}{k} D.$$

Computing the time derivative of $L_1(\tau)$ along the positive solution of (2.1) yields

$$\begin{aligned}
\frac{dL_1}{d\tau} &= -\frac{c}{T}(T - T^1)^2 + a_1 T^1 H^1 \left(3 - \frac{T^1}{T} - \frac{THW^1}{WT^1H^1} - \frac{H^1 W}{HW^1}\right) - \frac{g\nu D}{k} + gDW^1 \\
&= -\frac{c}{T}(T - T^1)^2 + a_1 T^1 H^1 \left(3 - \frac{T^1}{T} - \frac{THW^1}{WT^1H^1} - \frac{H^1 W}{HW^1}\right) + \frac{gD\nu}{k}\left(\frac{kcd}{a_1\alpha\nu p}(R_0^w - 1) - 1\right) \\
&= -\frac{c}{T}(T - T^1)^2 + a_1 T^1 H^1 \left(3 - \frac{T^1}{T} - \frac{THW^1}{WT^1H^1} - \frac{H^1 W}{HW^1}\right) + \frac{gD\nu}{k}(R_0^w - R_0^*).
\end{aligned}$$

Using the comparison between the arithmetical mean and the geometrical mean, we conclude that, if $1 < R_0^w \le 1 + \frac{a_1 p\alpha\nu}{dck}$, then, $dL_1/d\tau \le 0$ and L_1 is indeed a Lyapunov function for the equilibrium point EE^1. Moreover, it is straightforward that the largest compact invariant set contained in $\{(T, W, H, D) \in \mathbb{R}^4_+;\ dL_1/d\tau = 0\}$ is the singleton EE^1. By applying LaSalle's invariance Principle, the immunity-inactivated infection equilibrium EE^1 is globally asymptotically stable and unstable otherwise.

3. To prove the global asymptotic stability of $\widetilde{EE}^1$, we consider the following Lyapunov candidate:

$$L_3 = \left(T - \widetilde{T}^1 - \widetilde{T}^1 \ln \frac{T}{\widetilde{T}^1}\right) + \left(W - \widetilde{W}^1 - \widetilde{W}^1 \ln \frac{W}{\widetilde{W}^1}\right) + \frac{a_1 \widetilde{T}^1 \widetilde{H}^1}{p\alpha \widetilde{W}^1}\left(H - \widetilde{H}^1 - \widetilde{H}^1 \ln \frac{H}{\widetilde{H}^1}\right) + \frac{g}{k} D.$$

Direct computations lead to:

$$\begin{aligned}\frac{dL_3}{d\tau} &= -\frac{c}{T}(T - \widetilde{T}^1)^2 + a_1 \widetilde{T}^1 \widetilde{H}^1 \left(3 - \frac{\widetilde{T}^1}{T} - \frac{TH\widetilde{W}^1}{W\widetilde{T}^1\widetilde{H}^1} - \frac{\widetilde{H}^1 W}{H\widetilde{W}^1}\right) + gD\left(\widetilde{W}^1 - \frac{\nu}{k}\right) + 2\frac{a_1 \widetilde{T}^1 \widetilde{H}^1 f}{p\alpha \widetilde{W}^1} - \frac{a_1 \widetilde{T}^1 (\widetilde{H}^1)^2 f}{p\alpha \widetilde{W}^1 H} + H\left(a_1 \widetilde{T}^1 - \frac{a_1 \widetilde{T}^1 \widetilde{H}^1 d}{p\alpha \widetilde{W}^1}\right) \\ &= -\frac{c}{T}(T - \widetilde{T}^1)^2 + a_1 \widetilde{T}^1 \widetilde{H}^1 \left(3 - \frac{\widetilde{T}^1}{T} - \frac{TH\widetilde{W}^1}{W\widetilde{T}^1\widetilde{H}^1} - \frac{\widetilde{H}^1 W}{H\widetilde{W}^1}\right) + \frac{a_1 \widetilde{T}^1 \widetilde{H}^1 f}{p\alpha \widetilde{W}^1}\left(2 - \frac{\widetilde{H}^1}{H} - \frac{H}{\widetilde{H}^1}\right) + g\frac{gD}{a_1 kp\alpha}\left(ka_1 d\widetilde{H}^1 - (ka_1 f + pa_1 \alpha\nu)\right).\end{aligned}$$

Finally, by grouping terms, we have

$$\frac{dL_3}{d\tau} = -\frac{c}{T}(T - \widetilde{T}^1)^2 + a_1 T^1 H^1 \left(3 - \frac{\widetilde{T}^1}{T} - \frac{TH\widetilde{W}^1}{W\widetilde{T}^1\widetilde{H}^1} - \frac{\widetilde{H}^1 W}{H\widetilde{W}^1}\right) + \frac{a_1 \widetilde{T}^1 \widetilde{H}^1 f}{p\alpha \widetilde{W}^1}\left(2 - \frac{\widetilde{H}^1}{H} - \frac{H}{\widetilde{H}^1}\right) + \frac{g\nu D}{k}(\mathcal{T}_w - 1).$$

Therefore, using Lemma 1 above, if $R_w \leq 1$, then L_3 is actually a Lyapunov function for the equilibrium point $\widetilde{EE}^1$. Using LaSalle's invariance principle, we conclude that the immunity-inactivated infection equilibrium $\widetilde{EE}^1$ is globally asymptotically stable and unstable otherwise.

4. Following the same idea for $\widetilde{EE}^\sharp$, we consider the Lyapunov's candidate defined by:

$$L_4 = \left(T - \widetilde{T}^\sharp - \widetilde{T}^\sharp \ln \frac{T}{\widetilde{T}^\sharp}\right) + \left(W - \widetilde{W}^\sharp - \widetilde{W}^\sharp \ln \frac{W}{\widetilde{W}^\sharp}\right) + \frac{a_1 \widetilde{T}^\sharp \widetilde{H}^\sharp}{p\alpha \widetilde{W}^\sharp}\left(H - \widetilde{H}^\sharp - \widetilde{H}^\sharp \ln \frac{H}{\widetilde{H}^\sharp}\right) + \frac{g}{k}\left(D - \widetilde{D}^\sharp - \widetilde{D}^\sharp \ln \frac{D}{\widetilde{D}^\sharp}\right).$$

Direct computations and using equilibrium relations, one has:

$$\begin{aligned}\frac{dL_4}{d\tau} &= -\frac{c}{T}(T - \widetilde{T}^\sharp)^2 + a_1 \widetilde{T}^\sharp \widetilde{H}^\sharp \left(3 - \frac{\widetilde{T}^\sharp}{T} - \frac{TH\widetilde{W}^\sharp}{W\widetilde{T}^\sharp\widetilde{H}^\sharp} - \frac{\widetilde{H}^\sharp W}{H\widetilde{W}^\sharp}\right) + W\left(\frac{a_1 \widetilde{T}^\sharp \widetilde{H}^\sharp}{\widetilde{W}^\sharp} - p - g\widetilde{D}^\sharp\right) + 2\frac{a_1 \widetilde{T}^\sharp \widetilde{H}^\sharp f}{p\alpha \widetilde{W}^\sharp} - \frac{a_1 \widetilde{T}^\sharp (\widetilde{H}^\sharp)^2 f}{p\alpha \widetilde{W}^\sharp H} \\ &\quad + H\left(a_1 \widetilde{T}^\sharp - \frac{a_1 \widetilde{T}^\sharp \widetilde{H}^\sharp d}{p\alpha \widetilde{W}^\sharp}\right) + \frac{a_1 \widetilde{T}^\sharp \widetilde{H}^\sharp Hf}{p\alpha \widetilde{W}^\sharp \widetilde{H}^\sharp} - \frac{a_1 \widetilde{T}^\sharp \widetilde{H}^\sharp Hf}{p\alpha \widetilde{W}^\sharp \widetilde{H}^\sharp} \\ &= -\frac{c}{T}(T - \widetilde{T}^\sharp)^2 + a_1 \widetilde{T}^\sharp \widetilde{H}^\sharp \left(3 - \frac{\widetilde{T}^\sharp}{T} - \frac{TH\widetilde{W}^\sharp}{W\widetilde{T}^\sharp\widetilde{H}^\sharp} - \frac{\widetilde{H}^\sharp W}{H\widetilde{W}^\sharp}\right) + W\left(\frac{a_1 \widetilde{T}^\sharp \widetilde{H}^\sharp}{\widetilde{W}^\sharp} - p - g\widetilde{D}^\sharp\right) + \frac{a_1 \widetilde{T}^\sharp \widetilde{H}^\sharp f}{p_i \alpha \widetilde{W}^\sharp}\left(2 - \frac{\widetilde{H}^\sharp}{H} - \frac{H}{\widetilde{H}^\sharp}\right) \\ &= -\frac{c}{T}(T - \widetilde{T}^\sharp)^2 + a_1 \widetilde{T}^\sharp \widetilde{H}^\sharp \left(3 - \frac{\widetilde{T}^\sharp}{T} - \frac{TH\widetilde{W}^\sharp}{W\widetilde{T}^\sharp\widetilde{H}^\sharp} - \frac{\widetilde{H}^\sharp W}{H\widetilde{W}^\sharp}\right) + \frac{a_1 \widetilde{T}^\sharp \widetilde{H}^\sharp f}{p\alpha \widetilde{W}^\sharp}\left(2 - \frac{\widetilde{H}^\sharp}{H} - \frac{H}{\widetilde{H}^\sharp}\right).\end{aligned}$$

Again, the LaSalle's invariance principle is used to deduce the global asymptotic stability of the immunity-activated infection equilibrium $\widetilde{EE}^\sharp$.

6. Sensitivity analysis and simulation of the model

6.1. Sensitivity analysis

It is a common practice in mathematical immunology and epidemiology that sensitivity analysis informs how important each parameter is to the disease transmission outcomes, by determining how robust the model predictions (threshold numbers, variables, etc.) are to the parameter values. The ultimate aim of sensitivity analysis is to discover the model

Table 2
PRCCs of model 's variables.

Parameter	Range	PRCC (T)	PRCC (W)	PRCC (H)	PRCC (D)
π	[10–1000]	0.5312[a]	−0.0099	0.0074	0.1596
a	$[10^{-5}$–0.999]	−0.8758[a]	−0.0479	0.0276	0.6018[a]
c	[0.00104–0.999]	−0.7984[a]	0.0174	0.0025	−0.4103[a]
g	[0.00123–0.0055]	−0.0040	−0.0283	0.0056	−0.7863[a]
d	[0.048–2.5]	0.6024[a]	−0.0011	−0.9152[a]	−0.2293
p	[0.00092–0.99]	0.0083	−0.0322	0.0544	0.0217
f	[1–1000]	−0.8199[a]	0.0074	0.9707[a]	0.4097[a]
α	[10–1000]	−0.0136	−0.0136	0.0095	−0.0022
k	[0.00104–0.99]	0.0091	−0.9205[a]	−0.0377	0.7328[a]
ν	[0.00104–0.99]	−0.0032	0.9319[a]	0.0758	−0.7612[a]
e	[0.00104–0.99]	0.0577	−0.0338	−0.0044	−0.0266

[a] PRCC >0.4 and corresponding p-value <0.001.

parameters with high impacts on the infection outcomes and on which intervention/control strategies one should focus on. In this work, the sets of input parameter values are sampled using the Latin hypercube sampling (LHS) method and performing 1000 simulations to compute the partial rank correlation coefficients (PRCC) between each model parameter and the thresholds R_0^w, R_1^w, R_w and variables T, W, H, D (Marino et al., 2008). The results are summarised in Tables 2 and 3 and graphically represented in Fig. 3 and Fig. 4, while the most sensitive parameters are displayed in Table 4. We decide that a parameter in Table 2 is important/influential if the absolute value of PRCC is greater than 0.4 and its corresponding p-value is less than 0.001. The results in Table 2 show the PRCC values of the model variables. Table 3 presents the PRCC values for the threshold numbers R_0^w, R_1^w, R_w relative to the model parameters. From the sensitivity analysis using PRCC, the proliferation rate π of healthy epithelial cells mostly impacts healthy cells and has almost no influence on infected epithelial cells and HPV viruses. In addition, the proliferation rate π has a significant influence on the reproduction numbers R_1^w and R_w of immune cells, irrespective of whether there is activation of dormant HPV-infected cells (or provision of HPV viruses from external sources) or not. Similarly, the reproduction numbers R_1^w and R_w and the immune cells D are very sensitive to the density-dependent proliferation rate of immune cells k; the highest favourable influence being on the infected cells W. This is a desirable outcome because it shows that the higher the immune cells produced, the more the infected epithelial cells are killed. Another intuitive outcome of the sensitivity analysis is confirmed by the fact that the death rate of immune cells ν, has similar higher PRCC indexes (but with opposite signs) with respect to variables W and D. It is observable that, though the natural decay rate of viruses d is involved in the three threshold parameters R_0^w, R_1^w and R_w, it has a great influence solely on the basic reproduction number of infected cells R_0^w. Though all the model variables and thresholds depend on the burst size of infected viruses α, it is worth noticing that it has a low (or no) influence on them. No model variable is influenced by the apoptosis rate of infected cells p, which only has a relative impact on the reproduction number of immune cells R_w and no influence on R_1^w. It is understandable that the density-dependent death rate of infected cells g, does not appear in the expressions of any of the three threshold numbers, but it was not intuitive that only the immune cells D will be (highly) sensitive to that parameter. Although the constant activation rate f of dormant cells appears (which is expected and understandable) in the reproduction number of immune cells R_w, it does not have an influence on it; rather, it influences the densities of healthy epithelial cells and the HPV viruses, and to a lesser extent, the immune cells. This high influence of the reactivation of dormant cells f on T, H and D is further emphasized in Fig. 12, where higher values of f lead to lower values of T, higher values of H and D, but has no influence on the long term values of infected cells W. Noting that the efficacy rate of treatment (e) has a very low influence (PRCC $= 0.4062$) on the basic reproduction number R_0^w and no influence on the model

Table 3
PRCCs for model's thresholds.

Parameter	**Range**	**PRCC (R_w)**	**PRCC (R_1^w)**	**PRCC (R_0^w)**
π	[10–1000]	0.4544[a]	0.5861[a]	0.2804
a	$[10^{-5}$–0.999]	0.1134	−0.0552	0.4356[a]
c	[0.00104–0.999]	−0.0563	−0.4093[a]	/
g	[0.00123–0.0055]	/	/	/
d	[0.048–2.5]	−0.0313	0.0438	−0.4401[a]
p	[0.00092–0.99]	−0.4367[a]	−0.2982	/
f	[1–1000]	0.1082	/	/
α	[10–1000]	0.0035	−0.0497	0.3274
k	[0.00104–0.99]	0.4484[a]	0.4975[a]	/
ν	[0.00104–0.99]	−0.3676	−0.4465[a]	/
e	[0.00104–0.99]	−0.1470	−0.0167	−0.4062[a]

[a] PRCC >0.4 and the corresponding p-value <0.001.

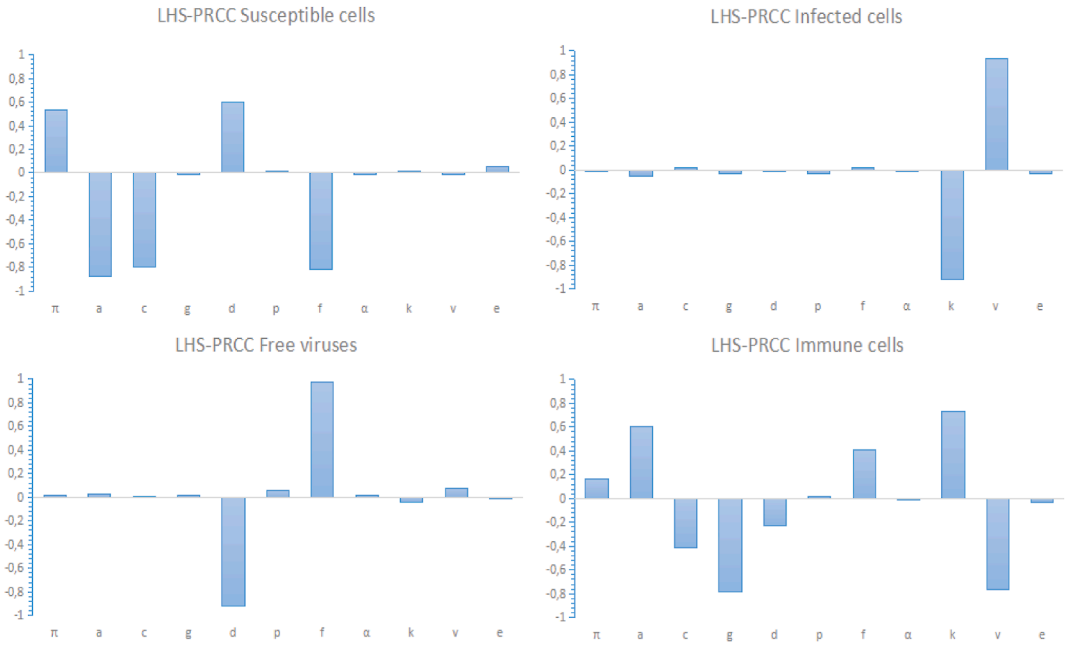

Fig. 3. LHS-PRCC Sensitivity analysis diagrams for the model's variables. From these diagrams, we observe that the parameter f has the highest sensitivity index, and has the highest impact on the HPV virus population H. The high sensitivity of infected cells to the proliferation and death rates of immune cells illustrates the cell-mediated immunity considered in this work. The susceptible cells are significantly sensitive to the parameters π, a, c, d and f. The immune cell variable D is sensitive to almost all the model parameters, compared to other variables.

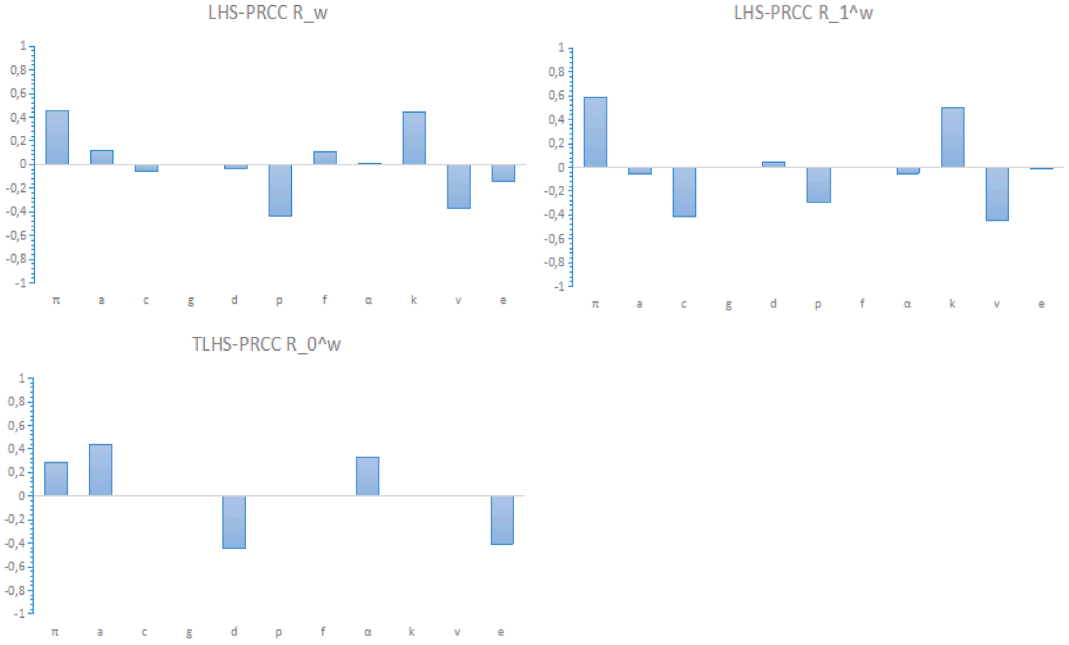

Fig. 4. LHS-PRCC Sensitivity analysis diagrams for the model's thresholds. From these plots, we notice that all the thresholds are sensitive to the parameter π in the same direction. An increase of k induces an increase in R_w and R_1^w as highlighting their biological interpretations.

variables is justified by the fact that, for HPV infection, there are only supportive treatments and no cure. Graphical plots of LHS-PRCC are presented below.

Table 4
Most influential parameters on model variables and thresholds (2.1).

Parameters	Π	a	c	g	d	p	f	α	k	ν	e
Sensitive variables	T	T, D	T	D	T, H		T, H, D		D	W, D	
Sensitive thresholds	R_w, R_1^w	R_0^w	R_1^w		R_0^w	R_w			R_w, R_1^w	R_1^w	R_0^w

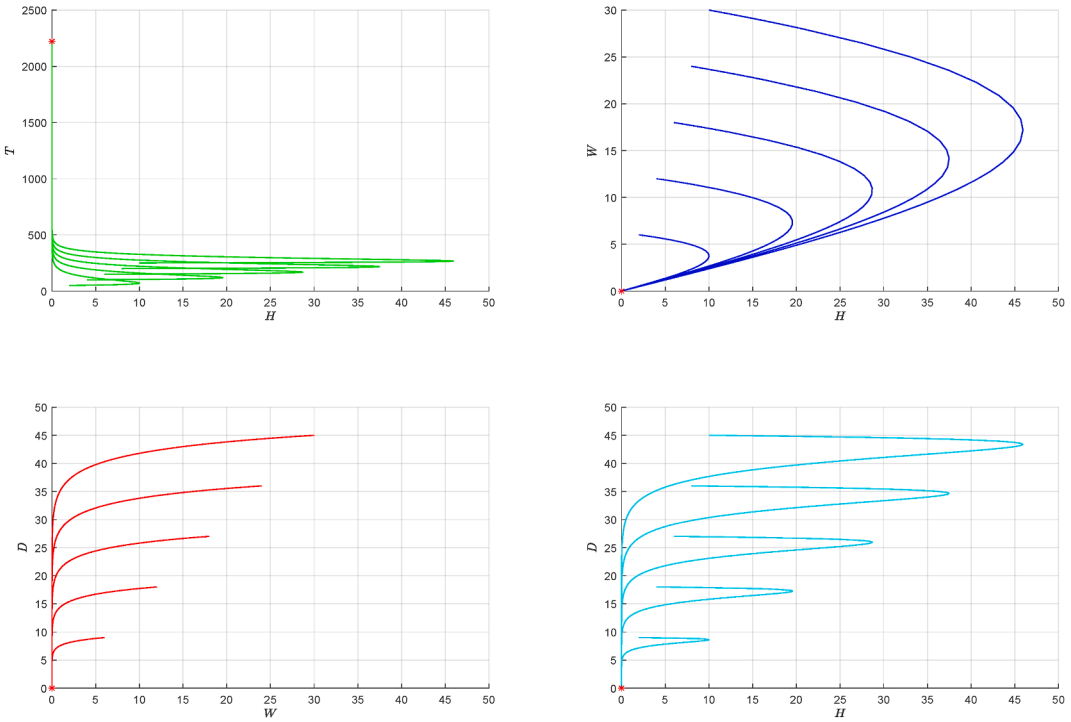

Fig. 5. Global Asymptotical Stability of the infection-free equilibrium (*IFE*): $R_0^w = 0.1422$.The parameters are: $\pi = 20$, $p = 0.4$, $c = 0.009$, $e = 0.04$, $a = 0.00001$; $\alpha = 10$, $g = 0.004401$, $d = 1.5$, $k = 0.0001045$, $\nu = 0.0412$, $f = 0$. This figure plots the trajectories of the system for many random intital conditions closer to the equilibrium point *IFE*, and shows that for a given set of parameters such that $R_0^w < 1$, then, irrespective of the initial condition, the corresponding trajectory tends to the unique equilibrium *IFE*. This proves that, irrespective of the initial viral, as long as model's parameters are such that $R_0^w < 1$, then the infection will ultimately be wiped out from the host, even in the case of a very poor (or absence of) immune response.

6.2. Simulations

In order to illustrate our theoretical results and highlight some important facts, we simulate the model (2.1). Most of the simulations carried out in this work are just to illustrate possible scenarios and theoretical results, and the parameters used are not necessarily derived from actual field data. However, insofar as possible, most of the parameters used in Table 1 are taken or estimated from trusted and relevant biological and mathematical references, as well as their upper and lower bounds. As demonstrated in Theorem 3 and Theorem 5, Figs. 5, 6 and 10 and 11, are provided to illustrate the local and global stability of the infection-free equilibrium, the immunity-inactivated equilibrium in the absence of reactivation of the dormant HPV-infected epithelial cell and the immunity-inactivated as well as immunity-activated equilibrium in the event of the reactivation of dormant HPV-infected epithelial cells, respectively. On the other hand, Figs. 8 and 9 show the existence of periodic solutions around the immunity-activated equilibrium in the absence of dormant HPV-infected cells, highlighting the presence of Hopf bifurcation as mentioned in Theorem 4. It can be seen in Fig. 8, that infected and immune cells increase simultaneously reaching a maximum, and starts the decreasing phase. In the increasing phase, infected cells dominate immune cells, whereas the situation reverses in the decreasing phase. These observations can be interpreted as follows: the increasing phase describes the period where infected cells and immune cells evolve independently (or the immune defence is absent or inefficient), while the decreasing phase may highlight the period during which immune cells interact with infected cells and dominate them.

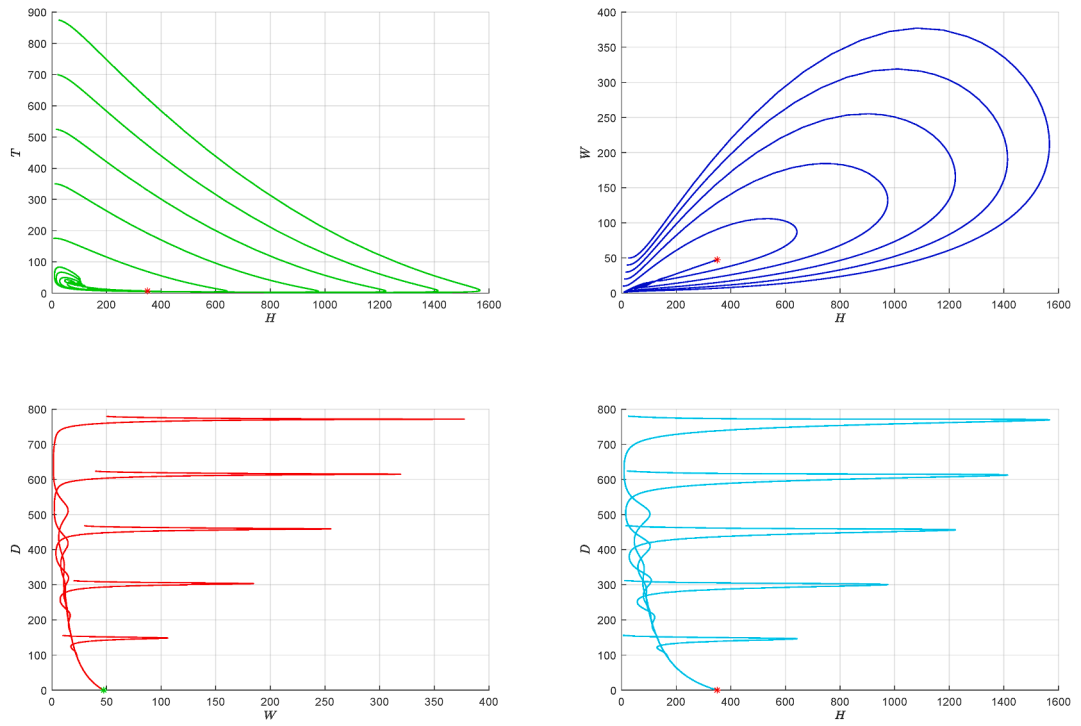

Fig. 6. Global asymptotical stability of the infection-free immunity-activated equilibrium (EE^1). Here $R_0^w = 311.7949$, $R_1^w = 0.12009$ are obtained using the following parameters: $\pi = 19$, $p = 0.4$, $c = 0.009$, $e = 0.2$, $a = 0.01$, $\alpha = 36$, $g = 0.004401$, $d = 1.95$, $k = 0.0001045$, $\nu = 0.0412$, $f = 0$. This figure plots the trajectories of the system for few intital conditions closer to the equilibrium point EE^1, and shows that for a given set of parameters such that $R_0^w > 1$ and $R_1^w < 1$, then, irrespective of the initial condition, the corresponding trajectory tends to the unique equilibrium EE^1, suggesting that the infection finally dies out while maintaining a vital immune response.

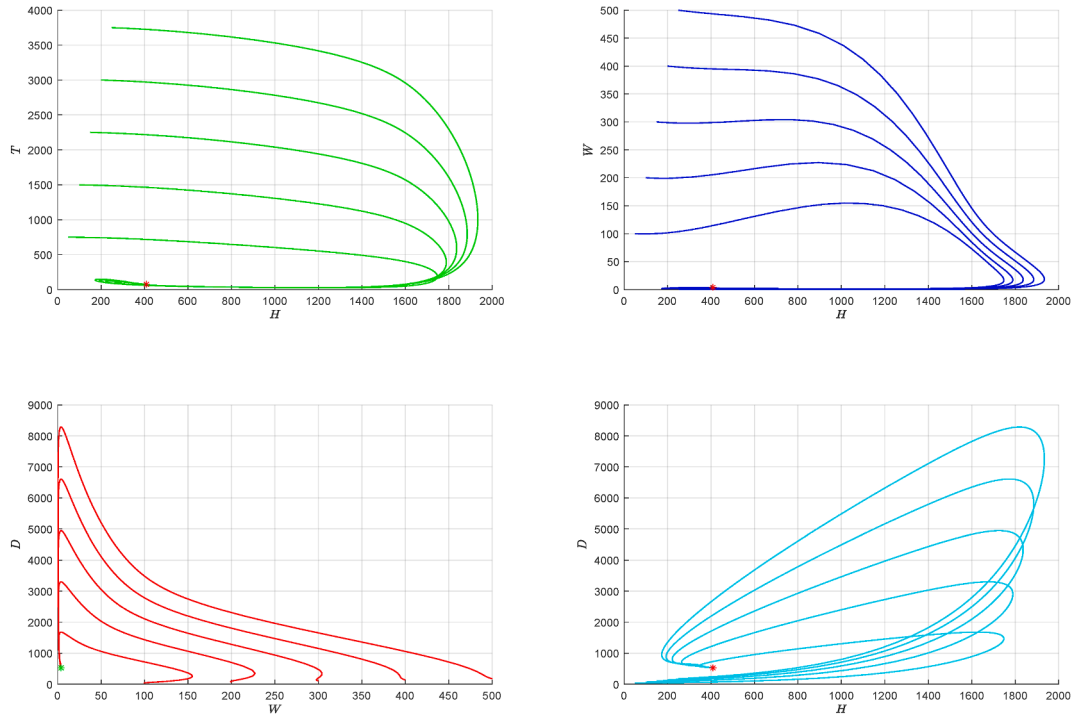

Fig. 7. Local asymptotic stability of $EE^\sharp$. Here $R_0^w = 720.00$, $R_1^w = 52.7684$ are obtained by using the following set of parameters: $\pi = 10$, $p = 0.048$, $c = 0.009$, $e = 0.7$, $a = 0.001$, $\alpha = 108$, $g = 0.004401$, $d = 0.05$, $k = 0.01045$, $\nu = 0.0412$, $f = 0$. This figure plots the trajectories of the system for many intital conditions around the equilibrium point $EE^\sharp$, and shows that for the above mentioned set of parameters such that R_0^w and R_1^w are greater than one, then the corresponding trajectory tends to the unique equilibrium point $EE^\sharp$, highlighting that the infection will persist in the long term with a vital immune response.

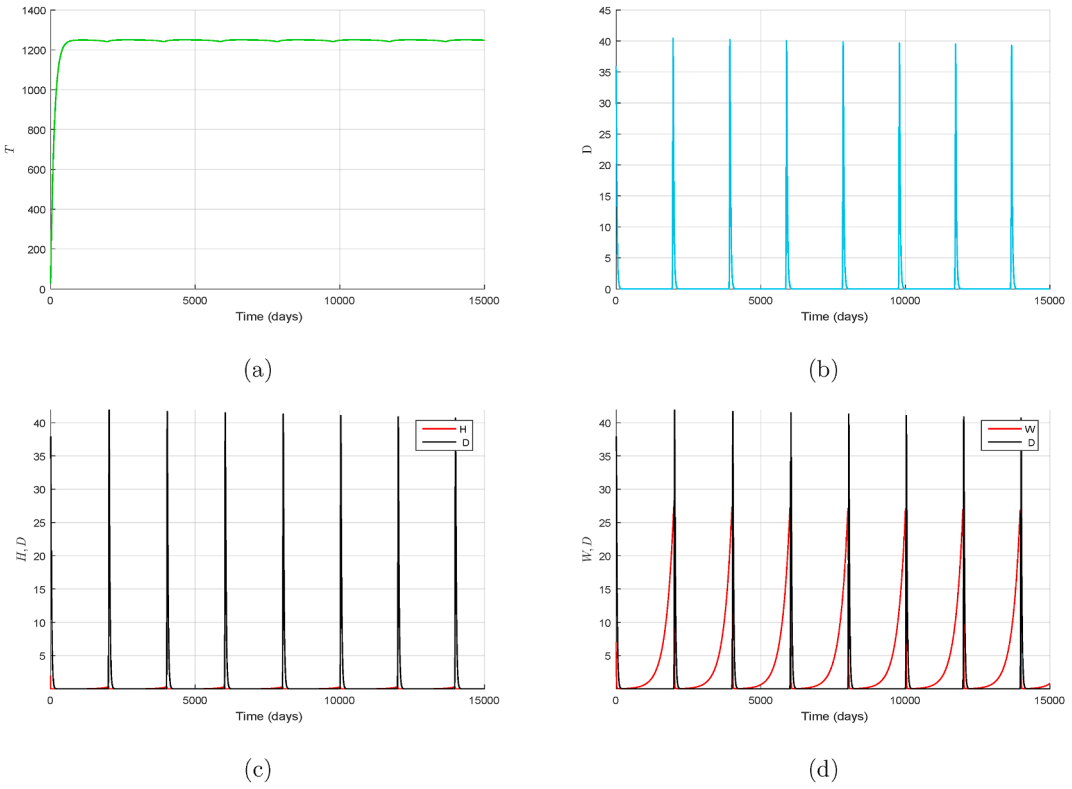

Fig. 8. Periodic solutions induced by $EE^{\sharp}$. Here $R_0^W = 38.5714$, $R_1^W = 24706.4905$ are obtained when the set of parameters: $\pi = 10$, $p = 0.0001$, $c = 0.001$, $e = 0.7$, $a = 0.001$, $\alpha = 108$, $g = 0.004401$, $d = 1.05$, $k = 0.01045$, $\nu = 0.0412$, $f = 0$. In this figure, the parameter values are chosen such that the local stability of the equilibrium is lost. This loss of stability gives rise to the occurrence of fluctuations in the state variables' values, which makes it more difficult to control the infection.

7. Discussion and conclusion

7.1. Discussion

There are at least three possibilities for adding cell dormancy and its reactivation in the model. The first is to add a recruitment rate of infected epithelial cells to the equation of infected cells. The second way is to assume a replenishment of the equation of viruses by some quantity of additional viruses. The last option is the combination of the first and the second, whereby one assumes the reactivation of infected dormant cells in the form of recruitment of infected cells, and the replenishment of free viruses in the equation of HPV viruses. However, for the sake of simplicity, we have opted for the second possibility, which indirectly accounts for the first option because (death) infected cells ultimately release free viruses.

Another main reason why we have chosen the second option is that it enables us to account for the situation whereby an infected person can get additional free viruses through unsafe sexual activities (rapes, unprotected sexual intercourse), environmental contamination and/or nosocomial infection. Based on this last reason, we were in some sense forced to use a constant recruitment of viruses, instead of a linear or any non-linear replenishment function of viruses.

Although we foresee that linear recruitment of free viruses will not significantly change the dynamics of the system, as long as the per-capita recruitment rate of viruses is less than its decay rate, it is worth mentioning that nonlinear recruitment functions may lead to completely different dynamics of the system. Therefore, our results and interpretations in this work are specific to the modelling assumptions adopted.

Human immunity is a very complex system and plays a pivotal role in the fight against viruses and other pathogen agents. It involves innate and adaptive immune responses, the former being non-specific and rapidly mounted as the first line of defence, while the latter is the adaptive immune response that is triggered whenever the innate fails. It is well known that humoral and cell-mediated immunity responses are two central types of adaptive immune response. Viruses spread in the human body through two different ways, one by virus-to-cell infection and the other by cell-to-cell transmission via direct contact. However, it is well documented that for HPV infection, the virus-to-cell transmission is the predominant mode of HPV dynamics, while the cell-to-cell transmission is almost absent (Murall et al., 2019).

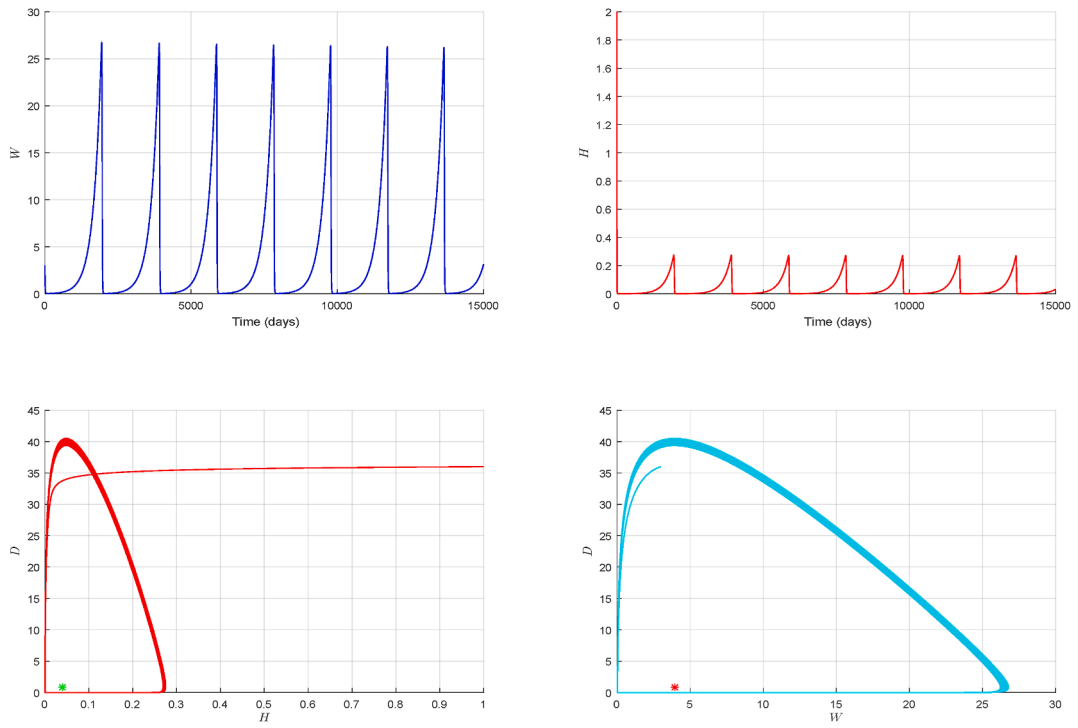

Fig. 9. Hopf bifurcation around $EE^{\sharp}$. Here $R_0^W = 38.5714$, $R_1^W = 24706.4905$ are obtained by using the following set of parameters: $\pi = 10$, $p = 0.0001$, $c = 0.001$, $e = 0.7$, $a = 0.001$, $\alpha = 108$, $g = 0.004401$, $d = 1.05$, $k = 0.01045$, $\nu = 0.0412$, $f = 0$. This figure complements Fig. 8 by representing phase portraits counterpart in some two-dimensional spaces so as to illutrate the occurrence of Hopf bifurcation.

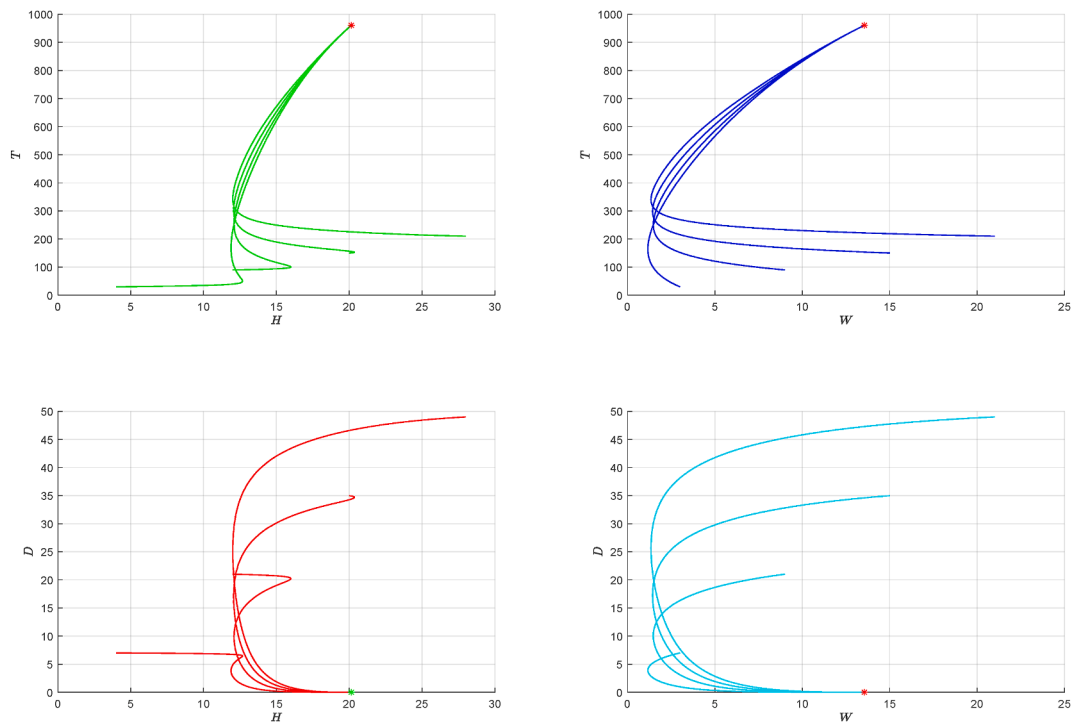

Fig. 10. Global asymptotical stability of $\widetilde{EE}^1$. Here $R_w = 0.57149$ (and $\mathcal{T}_w = 0.3435$) are obtained whenever: $\pi = 10$, $p = 0.1$, $c = 0.009$, $e = 0.3$, $a = 0.0001$ $\alpha = 15$, $g = 0.004401$, $d = 2.25$, $k = 0.01045$; $\nu = 0.0412$, $f = 25$. This figure plots the trajectories of the system for many random intital conditions and shows that for a given set of parameters such that $R_w < 1$ (and $\mathcal{T}_w < 1$), then, irrespective of the initial condition, the corresponding trajectory tends to the unique equilibrium $\widetilde{EE}^1$, highlighting that the infection will persist in the long term without an immune response.

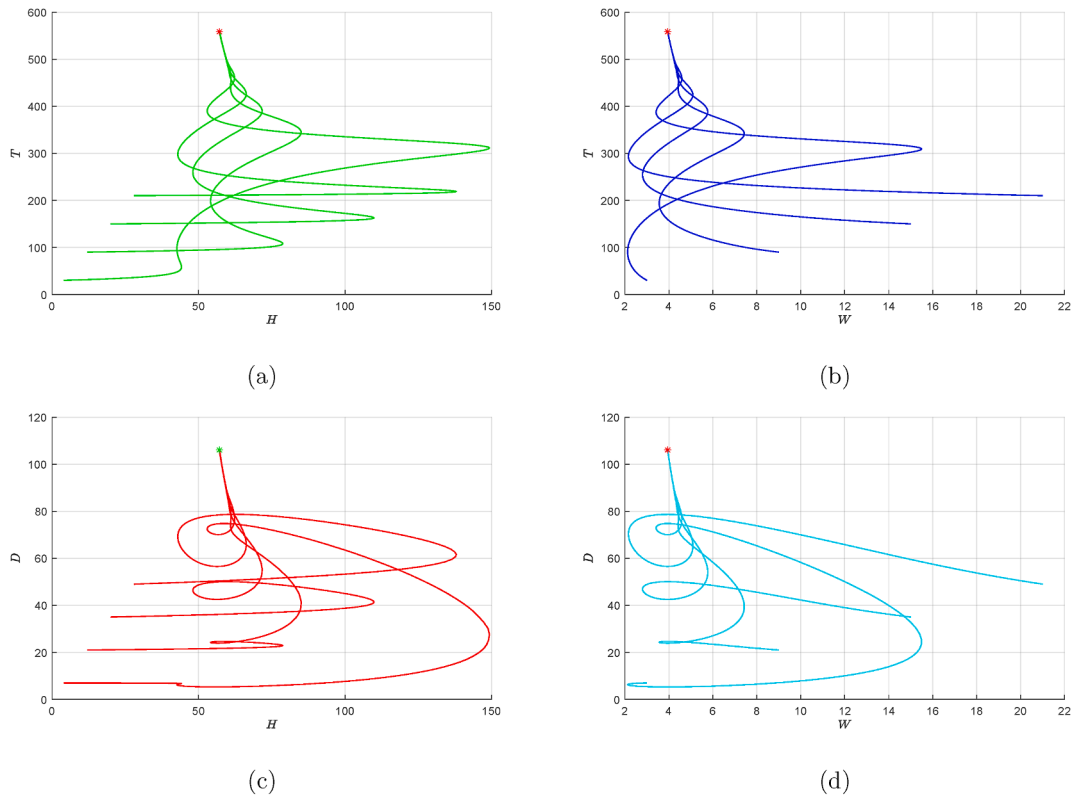

Fig. 11. Global asymptotical stability of $\widetilde{EE}^{\sharp}$ whenever $R_w = 5.6678$. The parameters are: $\pi = 10$, $p = 0.1$, $c = 0.009$, $e = 0.3$, $a = 0.0001$, $\alpha = 100$, $g = 0.004401$, $d = 1.25$, $k = 0.01045$, $\nu = 0.0412$, $f = 32$. This figure plots the trajectories of the system for many random intital conditions and shows that for a given set of parameters such that $R_w > 1$, then, irrespective of the initial condition, the corresponding trajectory tends to the unique equilibrium $\widetilde{EE}^{\sharp}$, suggesting that in this case, the infection will persist in the long term with an active immune response.

In our current model, without the reactivation of infected dormant cells, and applied to viral diseases with similar modes of transmission and immune defence systems, it is interesting to assess how its modified versions may behave when humoral immunity and other modes of transmission and their combinations are considered. In that perspective, considering the model with virus-to-cell transmission and humoral immune response does not change the behaviour of the model.

In fact, it has similar threshold parameters, the same number and types of equilibria, the same local and global stability results, and it also exhibits a Hopf bifurcation around the immunity-activated equilibrium (see Ref (Murase et al., 2005).). If one combines virus-to-cell and cell-to-cell modes of transmission with humoral immunity in a single model, the number and types of equilibria are preserved, and they are all globally asymptotically stable (see Ref (Pan & Chakrabarty, 2018).).

When two modes of transmission (virus-to-cell and cell-to-cell) of transmission and two types of immune responses (humoral and cellular) are considered, the same global asymptotic behaviour as in (Pan & Chakrabarty, 2018) is obtained (see (Hattaf & Yousfi, 2018)). These last two results preclude the existence of the Hopf bifurcation and is a huge behavioural change with our current model. When two modes of transmission (virus-to-cell and cell-to-cell) and two types of immune system (humoral and cellular immunity are considered in a single model, the same global asymptotic behaviour as in (Pan & Chakrabarty, 2018) is obtained (see (Hattaf & Yousfi, 2018)). These last two results preclude the existence of the Hopf bifurcation and are a huge behavioural change with our current model.

7.2. Conclusion and perspectives

In this paper, we presented an immunological model of HPV infection taking into account the role of immune defence and cell dormancy. We conducted a thorough analysis of the model and made major contributions in two main directions.

- From a theoretical perspective, we have analysed two sub-models.

For the sub-model without dormant cell reactivation or external free virus provision, the following analytical results were established.

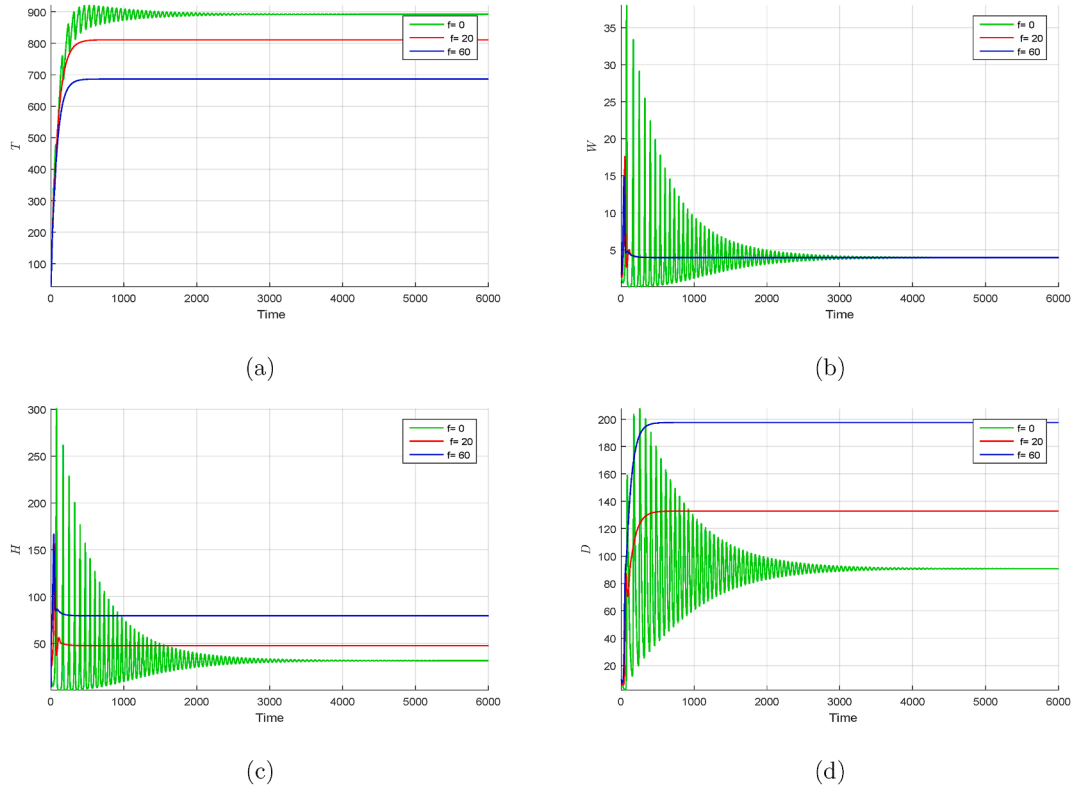

Fig. 12. Impact of dormant cells reactivation or external provision of free viruses on model variables. Here, three different values of the reactivation rate f is used as follows: $R_w(f=0)=4.9965$, $R_w(f=20)=6.8469$, $R_w(f=60)=9.6942$. The remaining parameters are chosen as: $\pi=10$, $p=0.1$, $c=0.009$, $e=0.3$, $a=0.0001$, $\alpha=100$, $g=0.004401$, $d=1.25$, $k=0.01045$, $\nu=0.0412$. From these plots, we observe that the parameter f prevents the occurrence of Hopf bifurcation, the same observation was made in (Blath & Tóbiás, 2021). In fact, the reactivation of dormant cells induces an increase in the viral load (c), which infects more susceptible cells (a) and triggers a higher immune response (d) to fight the infection. However, the observation that despite that fight, the population of infection cells stabilises at a nonzero value (b) shows the increase in f promotes the persistence of the infection.

– We explicitly determine the equilibrium points of the model based on the threshold parameters that were carefully extracted and interpreted.
– We have shown that the infection-free equilibrium and the immunity-inactivated equilibrium are locally asymptotically stable, using linearisation techniques and Routh-Hurwitz criteria.
– We have extended the local stability results of infection-free and immunity-inactivated equilibrium points to the global stability results using the Lyapunov and LaSalle techniques.
– As for the immunity-activated equilibrium point, we have established its local stability under conditions using the linearisation techniques and the Routh-Hurwitz criteria and showed that there is a possibility of Hopf bifurcation around this equilibrium.

For the sub-model with dormant cell reactivation or external free virus provision, we have shown the following results.

– Contrary to the sub-model without dormant cell reactivation or external free virus provision, this sub-model does not have the infection-free equilibrium; rather, it exhibits two equilibria, namely the immunity-inactivated and the immunity-activated equilibria, depending on the value of the explicitly determined threshold parameter R_w called "the reproduction number of immune cells".
– We have shown, using linearisation techniques and Routh-Hurwitz criteria, that the immunity-inactivated and immunity-activated equilibria are locally asymptotically stable.
– We have extended those local stability results to the global stability results using the Lyapunov and LaSalle techniques. This global stability precludes the existence of the Hopf bifurcation for the submodule with dormant cell reactivation or external free virus provision, making a big behavioural difference in the dynamics of the two sub-models.

• From the point of view of the numerical and sensitivity analysis, it is shown that:

- Reactivation of infected dormant cells can exacerbate the health condition of an infected person by promoting the persistence of infection, which further weakens the immune response and favours the progression of infection to HPV-induced cancers (see Fig. 12). This result is supported by the biological references (Song et al., 2015; Westrich et al., 2017; Wilkie & Hahnfeldt, 2013; Zhou et al., 2019).
- The bifurcation diagram for the full model was provided (see Fig. 2).
- The sensitivity analysis using PRCC showed that the proliferation rate π of healthy epithelial cells is the most influential parameter on healthy cells and has almost no influence on infected epithelial cells and HPV viruses. Moreover, it (π) had a significant influence on the reproduction numbers R_1^w and R_w of immune cells, irrespective of whether there is activation of dormant HPV-infected cells (or provision of HPV viruses from external sources) or not.
- Similarly, the reproduction numbers R_1^w and R_w, the immune cells D and infected cells (W) are very sensitive to the density-dependent proliferation rate k of immune cells; the highest favourable influence being on the infected cells W.
- The sensitivity analysis showed that the higher the immune cells produced, the more the infected epithelial cells are killed.
- An intuitive outcome of the sensitivity analysis is confirmed by the fact that the death rate of immune cells ν, has similar sensitivity index (but with opposite signs) with respect to infected cells W and immune cells D.
- It was not intuitive that solely immune cells D will be (highly) sensitive to the density-dependent death rate of infected cells g.
- Healthy epithelial cells, immune cells and HPV virus populations are highly sensitive to the activation rate f of dormant cells.
- The efficacy rate of treatment (e) had a very low influence on the basic reproduction number R_0^w and no influence on the model variables because there are only supportive treatments and no cure.

In its current form, the model developed in this work is easily transposable to other infections with a similar mode of transmission in the host. In particular, for viral (sexually transmitted) infections that induce cell dormancy and for which cell-mediated immunity prevails.

However, among the limitations of this work, we can emphasise the different ways of modelling the reactivation of infected dormant cells, the consideration of differential functional responses of infected cells when they are attacked by the immune cells, the differentiation between the innate immune system and the adaptive immune system, and the lack of theoretical proof of the existence of Hopf bifurcation. These drawbacks, among others, will be an avenue for future work.

An immediate perspective on which we are already actively working is to couple the current within-host model with a sex-structured population-level model of HPV dynamics by assuming that the provision (f) of free HPV viruses results from unsafe sexual activities with the opposite sex. Such a couple model will allow us to explore (using fast-slow dynamics) how the viral load of HPV generated at the individual level influences the transmission dynamics of HPV disease at the population level and vice versa.

CRediT authorship contribution statement

Michael Chapwanya: Writing – review & editing, Formal analysis, Conceptualization. **Adèle Claire Fouape:** Writing – review & editing, Formal analysis, Conceptualization. **Berge Tsanou:** Writing – review & editing, Formal analysis, Conceptualization.

Funding

This work was supported by the University of Pretoria Postdoctoral Program, South Africa; and the Bill & Melinda Gates Foundation-funded project CAFHOMEC (INV-059608), United States of America. Any opinions, findings, and recommendations expressed in this publication are those of the authors and do not necessarily reflect the views of the donors.

Declaration of competing interest

The authors declare that they have no known competing financial interests or personal relationships that could have appeared to influence the work reported in this paper.

Acknowledgements

Adèle Claire Fouape acknowledges the full support of the University of Pretoria#8217; s postdoctoral program. Michael Chapwanya and B. Tsanou acknowledge the financial support of the CAFHOMEC project funded by the Bill & Melinda Gates Foundation (INV-059608). The authors acknowledge and thank the two anonymous reviewers whose pertinent comments and suggestions have substantially improved the presentation of this manuscript.

References

Abate, A., Munshea, A., Nibret, E., Alemayehu, D. H., Alemu, A., Abdissa, A., Mihret, A., Abebe, M., & Mulu, A. (2025). Persistence and clearance rates of human papillomaviruses in a cohort of women treated or not treated for cervical dysplasia in northwest Ethiopia. *Scientific Reports, 15*(1), 8218.

Asih, T. S. N., Lenhart, S., Wise, S., Aryati, L., Adi-Kusumo, F., Hardianti, M. S., & Forde, J. (2016). The dynamics of HPV infection and cervical cancer cells. *Bulletin of Mathematical Biology, 78*, 4–20.

Blath, J., & Tóbiás, A. (2021). Virus dynamics in the presence of contact-mediated host dormancy. *arXiv preprint arXiv:2107.11242*.

Capasso, V., & Capasso, V. (1993). *Mathematical structures of epidemic systems, 97*. Springer.

Carter, J. J., Koutsky, L. A., Wipf, G. C., Christensen, N. D., Lee, S.-K., Kuypers, J., Kiviat, N., & Galloway, D. A. (1996). The natural history of human papillomavirus type 16 capsid antibodies among a cohort of university women. *Journal of Infectious Diseases, 174*(5), 927–936.

Chakraborty, S., Cao, X., Bhattyacharya, S., & Roy, P. (2019). The role of HPV on cervical cancer with several functional response: A control based comparative study. *Computational Mathematics and Modeling, 30*, 439–453.

Doorbar, J. (2023). The human papillomavirus twilight zone–latency, immune control and subclinical infection. *Tumour Virus Research, 16*, Article 200268.

Doorbar, J., Egawa, N., Griffin, H., Kranjec, C., & Murakami, I. (2015). Human papillomavirus molecular biology and disease association. *Reviews in Medical Virology, 25*, 2–23.

Gurcan, F., Kartal, S., Ozturk, I., & Bozkurt, F. (2014). Stability and bifurcation analysis of a mathematical model for tumor–immune interaction with piecewise constant arguments of delay. *Chaos, Solitons & Fractals, 68*, 169–179.

Hattaf, K., & Yousfi, N. (2018). Modeling the adaptive immunity and both modes of transmission in HIV infection. *Computation, 6*(2), 37.

Jensen, J. E., Becker, G. L., Jackson, J. B., & Rysavy, M. B. (2024). Human papillomavirus and associated cancers: A review. *Viruses, 16*(5), 680.

Lee, S. L., & Tameru, A. M. (2012). A mathematical model of human papillomavirus (HPV) in the United States and its impact on cervical cancer. *Journal of Cancer, 3*, 262.

Macfarlane, F. R., et al. (2019). *Mathematical modelling of tumour-immune competition tumour growth: Discrete and continuum approaches*. University of St Andrews. PhD thesis.

Mahlbacher, G. E., Reihmer, K. C., & Frieboes, H. B. (2019). Mathematical modeling of tumor-immune cell interactions. *Journal of Theoretical Biology, 469*, 47–60.

Marino, S., Hogue, I. B., Ray, C. J., & Kirschner, D. E. (2008). A methodology for performing global uncertainty and sensitivity analysis in systems biology. *Journal of Theoretical Biology, 254*(1), 178–196.

Murall, C. L., Jackson, R., Zehbe, I., Boulle, N., Segondy, M., & Alizon, S. (2019). Epithelial stratification shapes infection dynamics. *PLoS Computational Biology, 15*(1), Article e1006646.

Murase, A., Sasaki, T., & Kajiwara, T. (2005). Stability analysis of pathogen-immune interaction dynamics. *Journal of Mathematical Biology, 51*, 247–267.

Ntuli, L., Mtshali, A., Mzobe, G., Liebenberg, L. J., & Ngcapu, S. (2022). Role of immunity and vaginal microbiome in clearance and persistence of human papillomavirus infection. *Frontiers in Cellular and Infection Microbiology, 12*, Article 927131.

Pan, S., & Chakrabarty, S. P. (2018). Threshold dynamics of HCV model with cell-to-cell transmission and a non-cytolytic cure in the presence of humoral immunity. *Communications in Nonlinear Science and Numerical Simulation, 61*, 180–197.

RP, A. (2004). A history of the study of solid tumour growth: The contribution of mathematical modelling. *Bulletin of Mathematical Biology, 66*, 1039–1091.

Scott M, M. A., & Nakagawa, M. (2001). Cell-mediated immune response to human papillomavirus infection. *Clinical and Diagnostic Laboratory Immunology, 8*, 209–220.

Senba, M., & Mori, N. (2012). Mechanisms of virus immune evasion lead to development from chronic inflammation to cancer formation associated with human papillomavirus infection. *Oncology Reviews, 6*(2), e17.

Sierra-Rojas, J. C., Reyes-Carreto, R., Vargas-De-León, C., & Camacho, J. F. (2022). Modeling and mathematical analysis of the dynamics of HPV in cervical epithelial cells: Transient, acute, latency, and chronic infections. *Computational and Mathematical Methods in Medicine, 2022*(1), Article 8650071.

Smith, R. J., Li, J., Mao, J., & Sahai, B. (2013). Using within-host mathematical modelling to predict the long-term outcome of human papillomavirus vaccines. *Canadian Applied Mathematics Quarterly, 21*(2).

Song, D., Li, H., Li, H., & Dai, J. (2015). Effect of human papillomavirus infection on the immune system and its role in the course of cervical cancer. *Oncology Letters, 10*(2), 600–606.

Wang, M., Wang, Y., Hu, L., & Nie, L. (2024). Analysis of a delayed multiscale aids/hiv-1 model coupling between-host and within-host dynamics. *Axioms, 13*(3), 147.

Westrich, J. A., Warren, C. J., & Pyeon, D. (2017). Evasion of host immune defenses by human papillomavirus. *Virus Research, 231*, 21–33.

Wilkie, K. P., & Hahnfeldt, P. (2013). Mathematical models of immune-induced cancer dormancy and the emergence of immune evasion. *Interface Focus, 3*(4), Article 20130010.

Zhang, J., Ma, Y., Takeuchi, Y., Dong, Y., & Peng, Z. (2025). Modeling the media impact on the medication behavior of drug-sensitive patients in two-strain tuberculosis transmission and a case study. *SIAM Journal on Applied Dynamical Systems, 24*(2), 1494–1528.

Zhou, Y., Shi, X., Liu, J., & Zhang, L. (2023). Correlation between human papillomavirus viral load and cervical lesions classification: A review of current research. *Frontiers of Medicine, 10*, Article 1111269.

Zhou, C., Tuong, Z. K., & Frazer, I. H. (2019). Papillomavirus immune evasion strategies target the infected cell and the local immune system. *Frontiers in Oncology, 9*, 682.